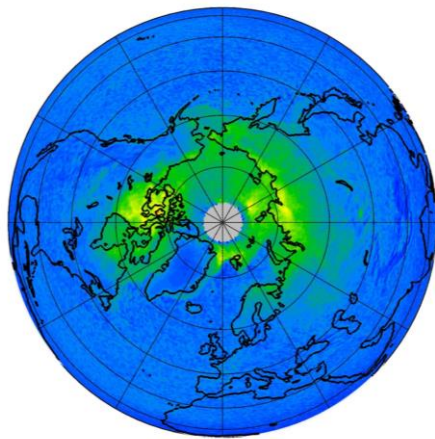


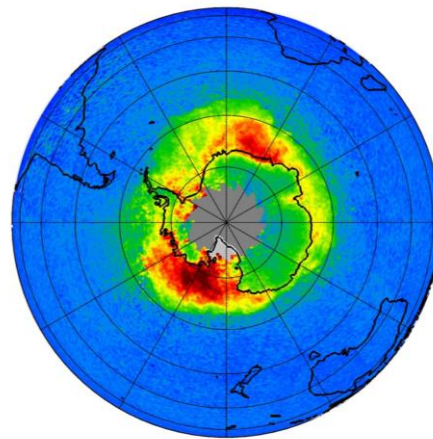
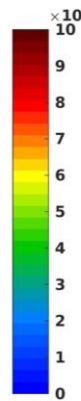
AC SAF VALIDATION REPORT

Validated products:

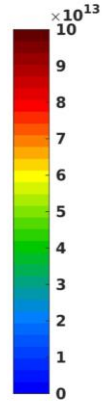
Name	Acronym
Tropospheric BrO Data Records from GOME-2 on Metop-A and Metop-B	O3M-116.0



Tropospheric BrO [molec.cm⁻²] March 2008



Tropospheric BrO [molec.cm⁻²] September 2008



Authors:

Name	Institute
Alexis Merlaud	Royal Belgian Institute for Space Aeronomy
Nicolas Theys	Royal Belgian Institute for Space Aeronomy
Jeroen van Gent	Royal Belgian Institute for Space Aeronomy
François Hendrick	Royal Belgian Institute for Space Aeronomy
Michel Van Roozendael	Royal Belgian Institute for Space Aeronomy
Udo Friess	University of Heidelberg
William R Simpson	University of Alaska Fairbanks
Klaus Peter Heue	German Aerospace Center

Reporting period: January 2007 – June 2020

Input data versions: GOME-2 Level 1B version 6.3

Data processor versions: G2_L2_BrOtrop, version 1.0

authors A. Merlaud, N. Theys, J. van Gent, F. Hendrick, Udo Friess, William R Simpson, K-P. Heue

edited by A. Merlaud, BIRA-IASB, Brussels, Belgium

reference SAF/AC/IASB/VR/CHOCHO/TN-IASB-GOME2AB-ACSAF-BrOTrop-2020
document type AC SAF Validation Report
issue 1
revision 0
date of issue 29-01-2022
products O3M-116.0
product version G2_L2_BrOtrop alg.version 1.0

distribution

Function	Organisation
AC SAF	EUMETSAT, BIRA-IASB, DLR, DMI, DWD, FMI, HNMS/AUTH, KNMI, LATMOS, RMI
UPAS Team	DLR-IMF, DLR-DFD
Ground-based data providers	BIRA-IASB, ChibaU

external contributors

contributing ground-based correlative measurements

Acronym	Organisation	Peoples
BIRA-IASB	Royal Belgian Institute for Space Aeronomy, Belgium	M. Van Roozendael, F..Hendrick, C. Fayt, C. Hermans
IUP-HD	University of Heidelberg, Institute of Environmental Physics	Udo Friess
UAF	University of Alaska Fairbanks	William R Simpson

document change record

Issue	Rev.	Date	Section	Description of Change
1	0	10.12.2020	All	Creation of this document
1	1	29.01.2022	All	Update of all the figures and texts due to a new version of the satellite product
1	2	02.03.2022	All	Update after review

AC SAF product ID numbers

AC SAF internal identifier	Description
Tropospheric BrO Data Record, GOME-2 Metop-A	O3M-116.0
Tropospheric BrO Data Record, GOME-2 Metop-B	O3M-116.0

Validation report of GOME-2 bromine monoxide tropospheric column data records for Metop-A and Metop-B

CONTENTS

ACRONYMS AND ABBREVIATIONS	4
INTRODUCTION TO EUMETSAT SATELLITE APPLICATION FACILITY ON ATMOSPHERIC COMPOSITION MONITORING (AC SAF)	5
DATA DISCLAIMER FOR THE METOP-A AND METOP-B GOME-2 TROPOSPHERIC BRO DATA RECORDS.....	7
A. INTRODUCTION.....	8
A.1. Scope of this document	8
A.2. Preliminary remarks	8
A.3. Plan of this document.....	9
B. ALGORITHM OVERVIEW.....	10
C. COMPARISONS WITH A SCIENTIFIC VERSION OF THE RETRIEVAL	12
D. CONSISTENCY BETWEEN GOME-2A AND GOME-2B.....	18
E. COMPARISONS WITH GROUND-BASED MEASUREMENTS	21
E1. Ground-based DOAS data sets description.....	21
E2. Coincidence criteria	22
E3. Comparison results in Arctic and at Harestua.....	23
E.3.1 Arctic MAX-DOAS measurements	23
E.3.2 Zenith-DOAS measurements in Harestua.....	25
E.3.3 Interpretation in terms of the product requirements.....	29
E4. Comparison results in Antarctica	32
CONCLUSIONS	35
F. REFERENCES	36
G.1. Applicable documents	36
G.2. Reference.....	36
G.2.1 Peer-reviewed articles	36
APPENDIX 1/ OPERATIONAL AND SCIENTIFIC ALGORITHM SETTINGS	38

ACRONYMS AND ABBREVIATIONS

AC SAF	Atmospheric Composition Monitoring Satellite Application Facility
AMF	Air Mass Factor, or optical enhancement factor
BIRA-IASB	Belgian Institute for Space Aeronomy
BrO	Bromine monoxide
DLR	German Aerospace Centre
DOAS	Differential Optical Absorption Spectroscopy
ESA	European Space Agency
EUMETSAT	European Organisation for the Exploitation of Meteorological Satellites
FRM4DOAS	Fiducial Reference Measurements for Ground-Based DOAS Air-Quality Observations
GDP	GOME Data Processor
GEOMS	Generic Earth Observation Metadata Standard
GOME	Global Ozone Monitoring Experiment
IMF	Remote Sensing Technology Institute
IUP-HD	Institute of Environmental Physics at the University of Heidelberg
LOS	Line Of Sight
MAXDOAS	Multi Axis Differential Optical Absorption Spectroscopy
MPC	Mission Performance Center
NDACC	Network for the Detection of Atmospheric Composition Change
O ₃	Ozone
OCRA	Optical Cloud Recognition Algorithm
OMI	Ozone Monitoring Instrument
QA4ECV	Quality Assurance for Essential Climate Variables
ROCINN	Retrieval of Cloud Information using Neural Networks
RRS	Rotational Raman Scattering
SCD	Slant Column Density
SNR	Signal to Noise Ratio
SZA	Solar Zenith Angle
TROPOMI	TROPOspheric Monitoring Instrument
UAF	University of Alaska Fairbanks
UPAS	Universal Processor for UV/VIS Atmospheric Spectrometers
UVVIS	Ultraviolet-visible spectrometry
VCD	Vertical Column Density
WMO	World Meteorological Organization

INTRODUCTION TO EUMETSAT SATELLITE APPLICATION FACILITY ON ATMOSPHERIC COMPOSITION MONITORING (AC SAF)

Background

The monitoring of atmospheric chemistry is essential due to several human-induced changes in the atmosphere, like global warming, loss of stratospheric ozone, increasing UV radiation, and pollution. Furthermore, it is used to react to threats caused by natural hazards as well as to follow the effects of international protocols.

Therefore, monitoring the chemical composition and radiation of the atmosphere is a very important duty for EUMETSAT and the target is to provide information for policy makers, scientists and general public.

Objectives

The main objectives of the AC SAF is to process, archive, validate and disseminate atmospheric composition products (O₃, NO₂, SO₂, BrO, HCHO, CHOCHO, H₂O, OClO, CO, NH₃), aerosol products and surface ultraviolet radiation products utilising the satellites of EUMETSAT. The majority of the AC SAF products are based on data from the GOME-2 and IASI instruments onboard Metop satellites.

Another important task besides the near real-time (NRT) and offline data dissemination is the provision of long-term, high-quality atmospheric composition products resulting from reprocessing activities.

Product categories, timeliness and dissemination

NRT products are available in less than three hours after measurement. These products are disseminated via EUMETCast, WMO GTS or internet.

- Near real-time trace gas columns (total and tropospheric O₃ and NO₂, total SO₂, total HCHO, CO) and high-resolution ozone profiles
- Near real-time absorbing aerosol indexes from main science channels and polarization measurement detectors
- Near real-time UV indexes, clear-sky and cloud-corrected

Offline products are available within two weeks after measurement and disseminated via dedicated web services at EUMETSAT and AC SAF.

- Offline trace gas columns (total and tropospheric O₃ and NO₂, total SO₂, total BrO, total HCHO, total H₂O) and high-resolution ozone profiles
- Offline absorbing aerosol indexes from main science channels and polarization measurement detectors
- Offline surface UV, daily doses and daily maximum values with several weighting functions

Data records are available after reprocessing activities from the EUMETSAT Data Centre and/or the AC SAF archives.

- Data records generated in reprocessing
- Lambertian-equivalent reflectivity
- Total OClO

Users can access the AC SAF offline products and data records (free of charge) by registering at the AC SAF web site.

More information about the AC SAF project, products and services: <https://acsaf.org/>

AC SAF Helpdesk: helpdesk@acsaf.org

Twitter: [https://twitter.com/Atmospheric SAF](https://twitter.com/Atmospheric_SAF)

DATA DISCLAIMER FOR THE METOP-A AND METOP-B GOME-2 TROPOSPHERIC BRO DATA RECORDS

In the framework of EUMETSAT's Atmospheric Composition Monitoring Satellite Application Facility (AC SAF), DLR produces the GOME-2 AC SAF data record of the bromine monoxide (BrO) tropospheric column from Metop-A and Metop-B GOME-2 measurements.

This report presents the verification of this AC SAF data record from Metop-A (2007-2018) and Metop-B (2012-2020) obtained with the G2_L2_BrOtrop processor and the v1.0 of the retrieval algorithm. BrO tropospheric column data were investigated through:

- 1) verification of their consistency with the BIRA-IASB scientific retrieval;
- 2) evaluation against ground-based observations from ground-based DOAS instruments.

The main results from the validation are summarized hereafter:

- The optimal requirements (30%) do not fit in the theoretical error budget.
- The AC SAF data record product is highly correlated with the BIRA scientific product, which covers the period between January 2007 and October 2009. The differences are mainly in the range of -0.5 to $+0.5 \times 10^{13}$ molec/cm² (mean difference of $+0.5 \times 10^{12}$ molec/cm²). This corresponds to relative differences in the range of -40 to $+50\%$ (mean difference of $+4\%$).
- Highest relative differences with respect to the scientific product on the DLR tropospheric BrO VCDs mostly occur in background areas and Antarctica.
- GOME-2A and GOME-2B data are generally consistent in terms of seasonal and latitudinal changes. However, the GOME-2A time series seems to change from 2014, possibly due to instrumental degradation.
- The GOME-2 BrO VCDs shows a good correlation with the ground-based DOAS measurements in Arctic. Linear regression analyses between the two products typically yield slopes close to unity, however there remains a positive bias of the GOME-2 VCDs. The limitation of the MAX-DOAS technique in the free troposphere makes it difficult to quantify accurately the bias. Assuming 1×10^{13} molec/cm² in the free troposphere leads to a positive bias of around 70%, which is close to the target requirements
- In Harestua, the average positive bias in the considered period (2013-2020) is 84% and 1%, respectively for GOME-2A and GOME-2B.
- It appears difficult to interpret comparisons between GOME-2 and MAX-DOAS data in Antarctica. However, previous studies suggests that, in this area, a large fraction of the column is present in the free troposphere, where the MAX-DOAS is not sensitive.
- Overall, with respect to the available validation data, GOME-2A and GOME-2B seem to comply with the threshold requirements of 100% and appear close to the target requirements of 60%.

A. INTRODUCTION

A.1. Scope of this document

The present document reports on the verification and geophysical validation of GOME-2/Metop-A tropospheric BrO column data acquired over the 2007-2020 period and GOME-2/Metop-B data acquired over the 2012-2020 period. The data were produced by the GOME Data Processor G2_L2_BrOTrop operated at the DLR Remote Sensing Technology Institute (DLR-IMF, Oberpfaffenhofen, Germany) in the framework of the EUMETSAT AC SAF. This report addresses the verification of the operational Metop-A and Metop-B tropospheric BrO data records. This is achieved by comparing first the DLR operational product with a BIRA-IASB scientific version using the same level 1 data and then with ground-based MAX-DOAS reference data sets in the Arctic Ocean and in Harestua (Norway). The goal is to investigate the overall consistency of the GOME-2 tropospheric BrO data records and to assess whether the product fulfils the user requirements in term of accuracy (threshold 100%, target 60% and optimal 30% for polluted conditions), as stated in the ACSAF Product Requirement Document.

Optimal for bromine explosion events	30%
Target	60%
Threshold	100%

Table A.1 Requirements for the GOME-2 tropospheric BrO VCDs

A.2. Preliminary remarks

We use several sets of ground-based DOAS measurements from different field campaigns. The measurements in the Arctic were performed with the same type of instruments (MAX-DOAS) from two groups (IUP-HD and UAF) with stationary instruments and from moving platforms on the Arctic Ocean. As will be mentioned again below, MAX-DOAS measurements are mainly sensitive to the lower troposphere, i.e. the BrO column density between the surface and 2 km. We thus added a ghost column based on the known BrO content in the free troposphere. The uncertainty on this assumption adds up to the errors on the MAX-DOAS VCD itself, so the biases we report below should not be overinterpreted.

A.3. Plan of this document

This document is divided in five main parts. We first (section B) describe the algorithm used to retrieve tropospheric BrO VCDs from GOME-2 measurements. We then (section C) compare the operational product with a scientific version of the algorithm, using the same general approach but with different settings. Section D investigates the consistency between GOME-2A and GOME-2B. Section E compares the operational product with ground-based measurements. This is followed by concluding remarks and perspectives for future work.

B. ALGORITHM OVERVIEW

The tropospheric BrO vertical column densities (VCD_{tropo}) are retrieved using a residual technique (Theys et al., 2011) according to the following equation:

$$VCD_{\text{tropo}} = \frac{SCD - VCD_{\text{strato}} \cdot AMF_{\text{strato}}}{AMF_{\text{tropo}}} \quad (1)$$

The approach consists of three main steps:

1. A slant column density (SCD) is determined from calibrated earth-shine and irradiance spectra using a DOAS fit. This slant column is a “total” SCD in the sense that it includes contributions from absorption by BrO in both the stratosphere and troposphere. To correct for possible stripes and offsets in the data a normalization of the data is implemented based on daily averaged equatorial SCDs.
2. The stratospheric vertical column (VCD_{strato}) is estimated using simulated stratospheric BrO profiles from a climatological approach driven by O₃ and NO₂ observations.
3. The residual tropospheric vertical column is obtained by applying stratospheric and tropospheric air mass factors (AMF_{strato} and AMF_{tropo}) to account for changes in measurement sensitivity in both stratosphere and troposphere.

An error assessment of the BrO columns is presented in the table below. It is interesting to compare the tropospheric BrO accuracy (last line of the table below) with the product requirements in Section A.1. The optimal requirements (30%) do not appear reachable. Moreover, the target and threshold requirements should apply to different conditions, respectively polar and mid-latitude.

Error source	Error Total column	Error Tropospheric column
BrO slant column		
BrO absorption cross-sections	5-10%	5-10%
Instrument signal-to-noise	10-20%	10-20%
Stratospheric BrO column	n.a.	20%
BrO equatorial correction	1×10^{13} molec/cm ² / AMF_{total} (absolute error)	1×10^{13} molec/cm ² / AMF_{tropo} (absolute error)
BrO Air Mass Factor	10-25% (polar/tropics-mid.lat.)	20-50% (polar/ tropics-mid.lat.)
BrO vertical column (accuracy)	20/30%	35/55%

Table B.1 Estimation of error sources for the total and tropospheric BrO column.

As noted above, the operational implementation (referred as ‘oper’ in the following) is based on a scientific algorithm (hereafter referred as ‘scient’) developed by BIRA-IASB (Theys et al., 2011). However, different practical choices between oper and scient settings exist and are summarized in the Table given in Appendix 1, separately for each of the retrieval steps (i.e. right-hand terms of Eq. 1 above). Note that for the operational implementation, changes have been made to improve

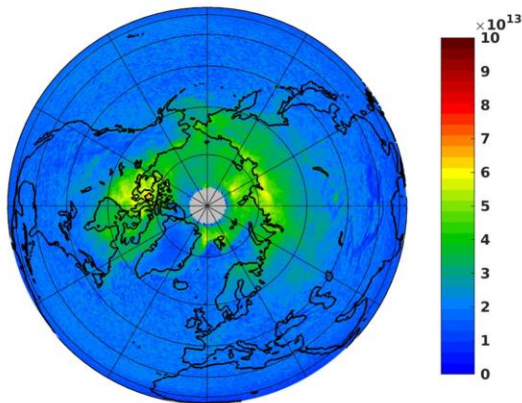
the results. For instance for the surface albedo, the scient set-up uses the GOME-1 data from Koелеmeijer et al. (2003) while oper uses Tilstra et al. (2017), a more adequate set-up for GOME-2. The cloud products are also different, as well as the treatment of snow/ice scenes. Therefore, differences are expected in the AMFs but it is not clear which set-up is better.

C. COMPARISONS WITH A SCIENTIFIC VERSION OF THE RETRIEVAL

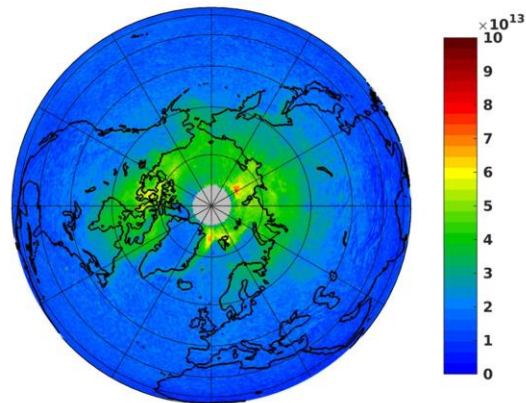
Here, the scientific and operational retrievals are compared for GOME-2A for nearly 3 years, from January 2007 to October 2009.

As a first comparison, Figure C.1 shows monthly averaged maps from oper and scient for polar spring in both hemispheres. As can be seen, the tropospheric BrO column distributions are similar for both datasets. In the Northern hemisphere, there is no obvious tendency for oper data to over/underestimate the scient values. For the Southern hemisphere, oper data tends to have slightly higher columns than scient. over the Antarctic continent and lower background at mid-latitudes. Note also that oper. seems much less affected by the South Atlantic Anomaly (SAA) than the scient. results.

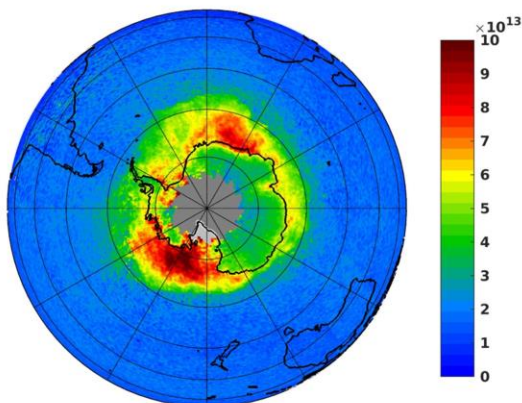
GOME-2A Oper BrO Tropo VCD (molec.cm-2) 2008.03



GOME-2A Scient BrO Tropo VCD (molec.cm-2) 2008.03



GOME-2A Oper BrO Tropo VCD (molec.cm-2) 2008.09



GOME-2A Scient BrO Tropo VCD (molec.cm-2) 2008.09

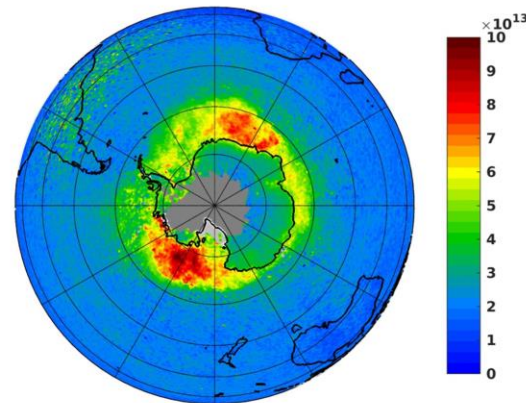
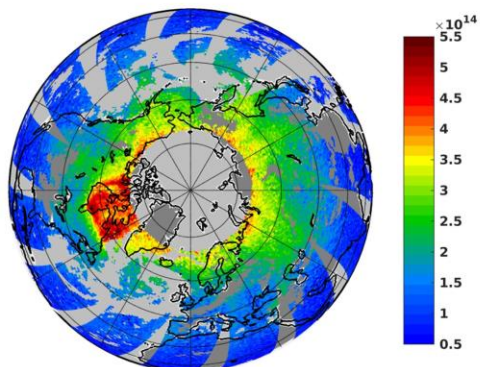


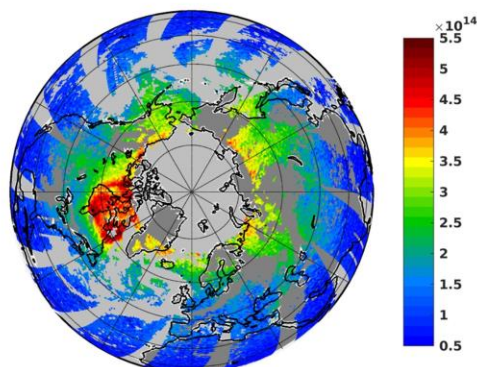
Figure C.1: Comparison of monthly averaged tropospheric BrO columns from oper (left) and scient (right) algorithms for Northern high-latitudes in March 2008 (top) and Southern high-latitudes in September 2008 (bottom).

In order to further investigate the final BrO product, Figures C.2 and C.3 show the results (as an example for the 25th Feb 2008 in the Northern hemisphere) of tropospheric BrO VCD and from the different algorithmic steps (see Eq. 1) for oper and scient: total SCD, stratospheric VCD, stratospheric AMFs, tropospheric AMFs, as well as the surface albedo used. One can conclude from Figures C.2 and C.3 that the stratospheric AMFs are in very good agreement but the stratospheric VCDs are quite different, likely because of different definition of the tropopause. At first glance, the BrO SCDs are also close but not identical. Finally, rather large differences are observed in the tropospheric AMFs with scient being large than oper values. This feature is not unexpected because of a number of differences in the input data (see summary table in the appendix 1). For instance, the pixel selection is not the same because different cloud products are used. In Figure C.3, it is clear that surface albedos are also not the same, however the difference is not systematic. While the albedos used in oper generally appears larger, the opposite holds true in some important areas, like around the Hudson Bay where elevated BrO VCDs are observed this day, with lower AMFs and albedos of the oper product around this area. Finally, the different profiles in the two product versions explain the difference for the low-albedo scenes. Over these areas, the scient AMF assumes a constant BrO concentration in the free troposphere. It is therefore higher than the oper AMF which assumes all tropospheric BrO under 2.5 km altitude. On this day and compared to the scient product, the lower AMFs of the oper product seem to compensate for its larger stratospheric VCDs.

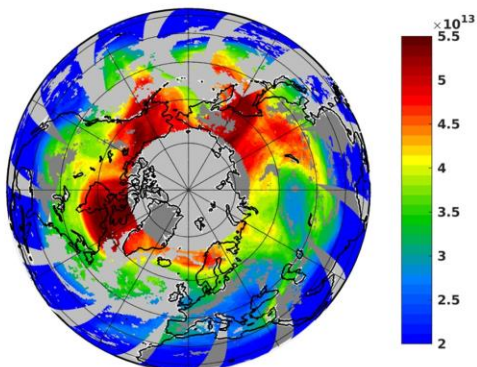
GOME-2A Oper BrO SCD (molec.cm-2) 2008.02.25



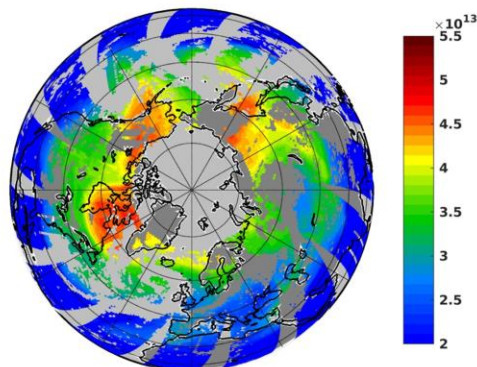
GOME-2A Scient BrO SCD (molec.cm-2) 2008.02.25



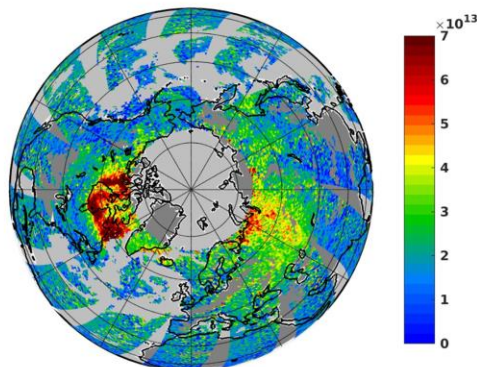
GOME-2A Oper BrO Strato VCD (molec.cm-2) 2008.02.25



GOME-2A Scient BrO Strato VCD (molec.cm-2) 2008.02.25



GOME-2A Oper BrO Tropo VCD (molec.cm-2) 2008.02.25



GOME-2A Scient BrO Tropo VCD (molec.cm-2) 2008.02.25

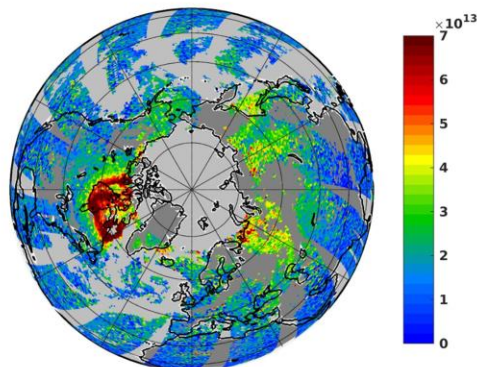
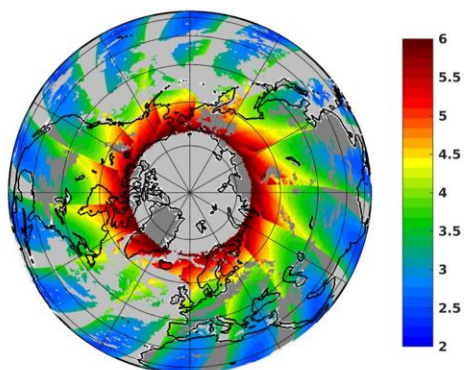
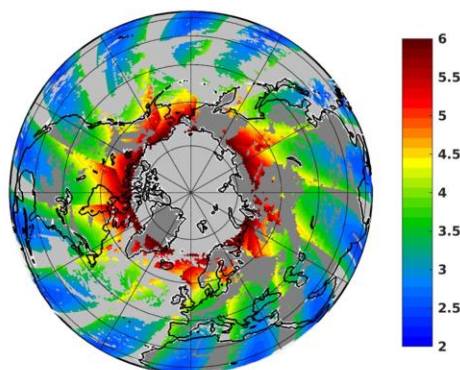


Figure C.2: Comparison of results from oper (left) and scient (right) algorithms for Northern high-latitudes on 25th February 2008, from top to bottom: BrO slant columns, stratospheric VCD and tropospheric VCD.

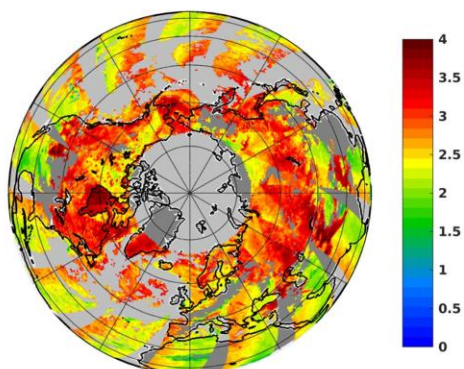
GOME-2A Oper BrO Strato AMF (-) 2008.02.25



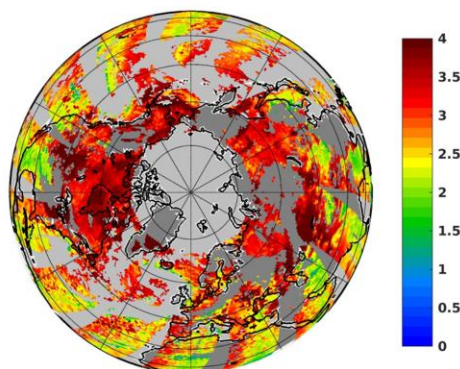
GOME-2A Scient BrO Strato AMF (-) 2008.02.25



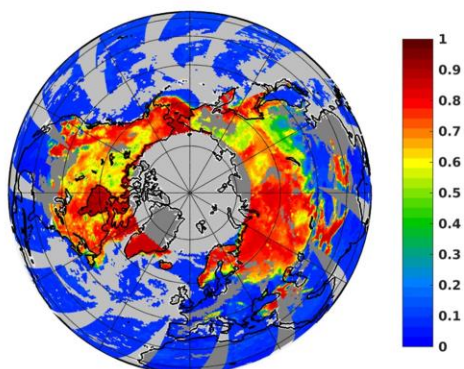
GOME-2A Oper BrO Tropo AMF (-) 2008.02.25



GOME-2A Scient BrO Tropo AMF (-) 2008.02.25



GOME-2A Oper BrO Albedo (-) 2008.02.25



GOME-2A Scient BrO Albedo (-) 2008.02.25

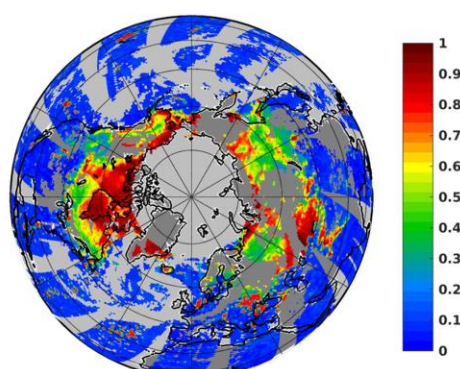


Figure C.3: same as Fig. C.2, from top to bottom: stratospheric AMF, tropospheric AMF and surface albedo.

In Figure C.4, time-series of tropospheric BrO columns from oper and scient are compared for different 5° zonal bands (from pole-to-pole) and over the period from January 2007 to October 2009; the absolute and relative differences are also displayed. The oper tropospheric VCDs differ from scient by values up to 10^{13} molec/cm² in absolute values (at high latitudes or at southern latitudes) but generally in the range of -0.5 to $+0.5 \times 10^{13}$ molec/cm², with a mean difference of

$+0.5 \times 10^{12}$ molec/cm². This corresponds to relative difference in the range of -40 to +50%, and a mean difference of +4%.

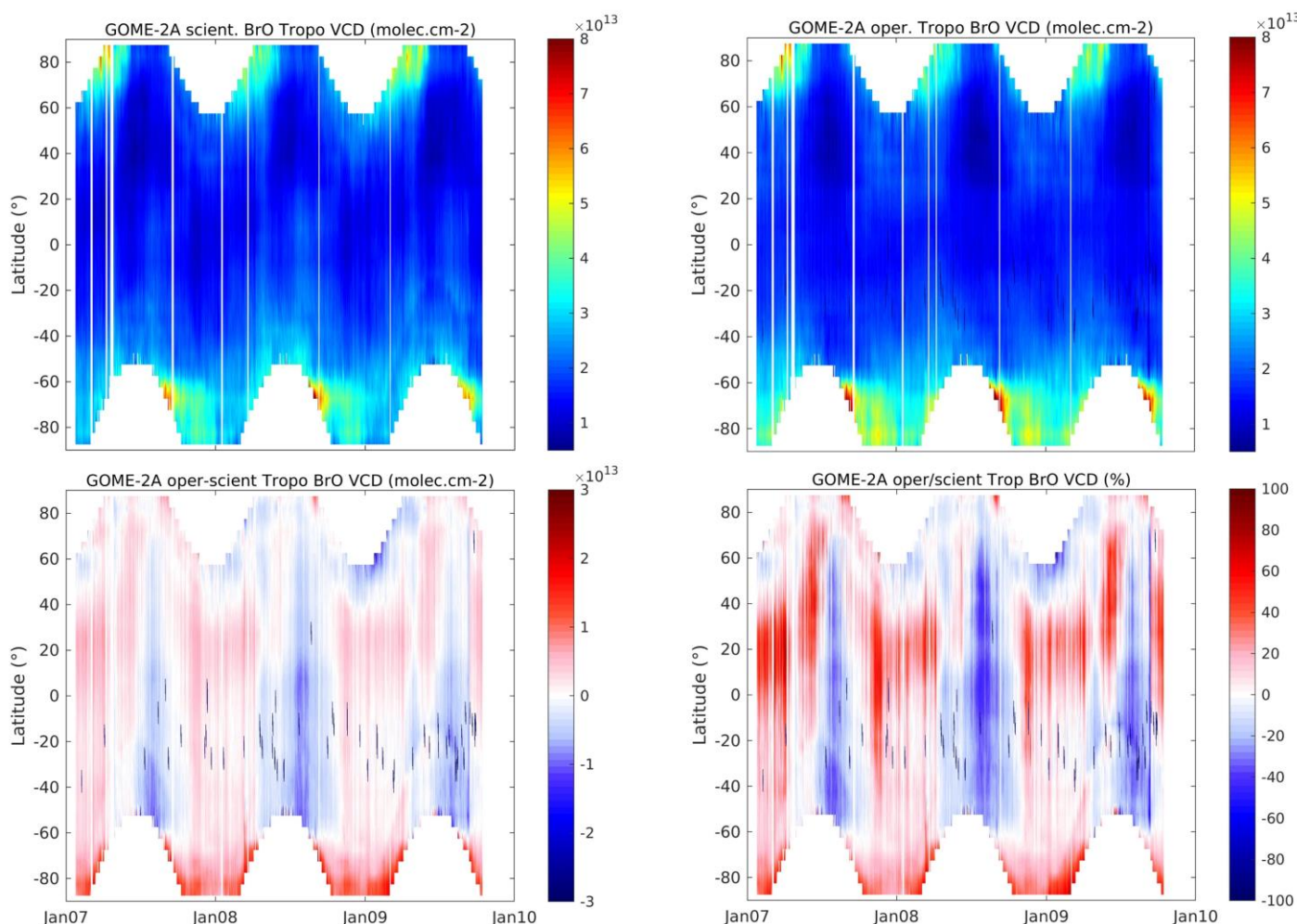


Figure C.4: Comparison of time-series of daily averaged tropospheric BrO columns (for 5° zonal bands) from scient (upper left) and oper (upper right) algorithms. The absolute and relative differences (oper minus scient) are displayed in bottom panels.

Figure C.5 provides additional information on the origin of the differences with time-series of relative differences for BrO SCDs, tropospheric SCDs, tropospheric AMFs, stratospheric VCDs and stratospheric AMFs (similar as Fig. C.4). From Figure C.5, it is found that the stratospheric correction contributes of -5% to +15% (average: +5%) to the observed differences in the tropospheric BrO VCDs. The oper tropospheric BrO AMFs are ~ -5% to -15% (average: -9%) lower than scient. The total BrO SCDs of oper and scient are found different by -5% to +10% (average: +2%). However, it should be stressed that any error in BrO SCD propagates to the tropospheric BrO columns with a multiplying factor of AMF_{strato}/AMF_{tropo} which is often larger than one.

From Fig C5, it is interesting to note that even if the differences in the tropospheric BrO VCDs have significant time and zonal variations, this seems to be much less the case for the intermediate products (SCD, stratospheric correction and tropospheric AMFs) which vary mostly in time and not so much with latitude. For example, the SCDs tend to be lower in late summer-autumn (August to October) and higher mostly for the other months of the year. This could be related to difference in the reference spectrum used or offset corrections. For the tropospheric AMFs, the underestimation is systematic for all months but more pronounced in winter, possibly because of

differences in the albedos used. For the stratospheric VCDs, higher values than scient. are systematically found for March-June.

However, the differences of the intermediate steps are generally fairly modest (less than 15% in absolute values). The resulting relative differences on the final tropospheric BrO VCDs can be substantial but this mostly occurs for months-latitudes with low column values (background).

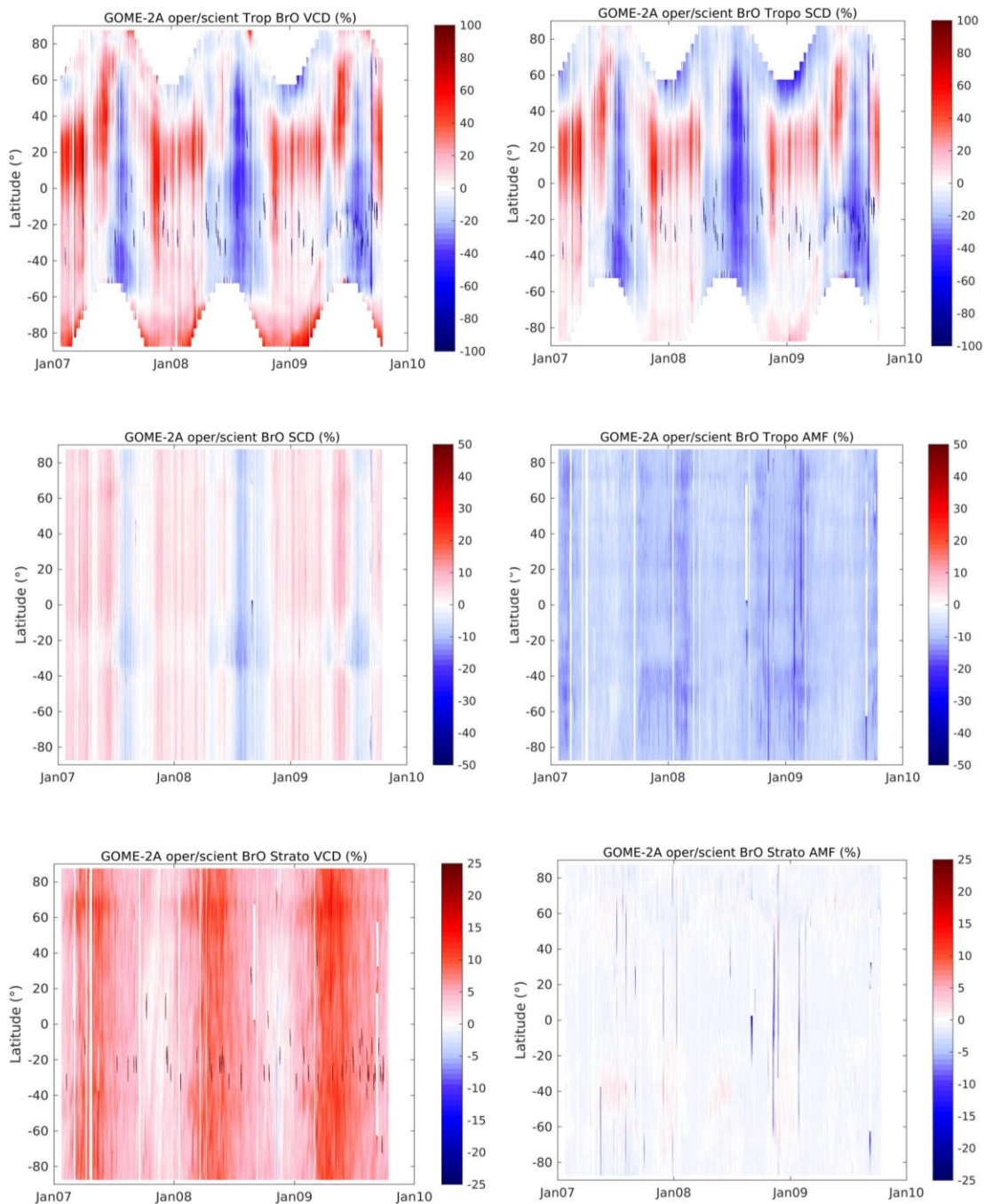
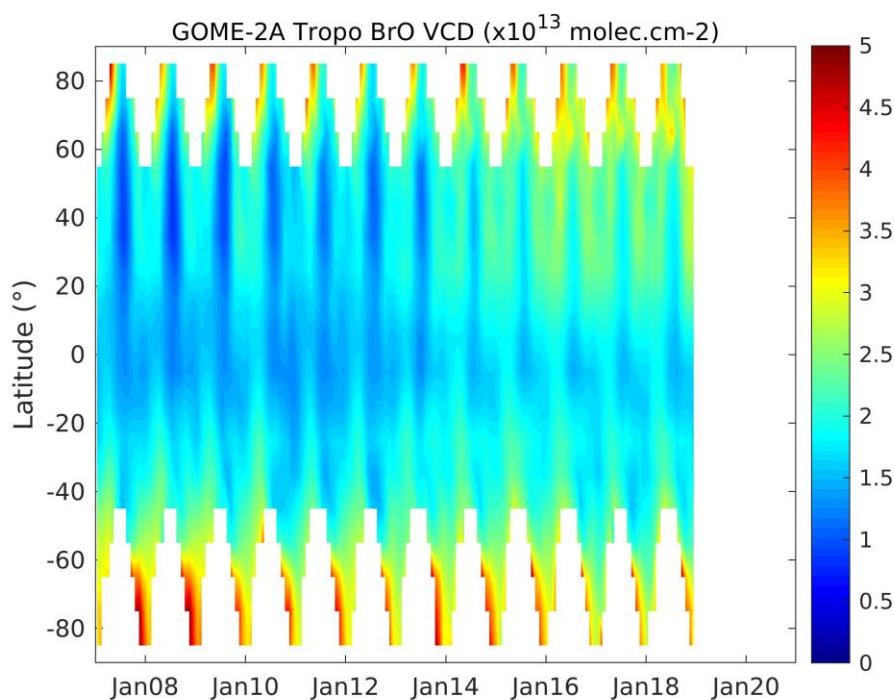


Figure C.5: Comparison of time-series of daily averaged relative differences (oper minus scient) for BrO Tropospheric VCDs, BrO Tropospheric SCDs, BrO total SCDs, tropospheric AMFs, stratospheric VCDs and stratospheric AMFs (for 5° zonal bands).

D. CONSISTENCY BETWEEN GOME-2A AND GOME-2B

The consistency between GOME-2A and GOME-2B tropospheric BrO VCDs is investigated in Fig. D.6 and Fig. D.7 (top panel) through time-series of monthly zonal averages for the period of 2007-2020. As can be seen, the GOME-2A and GOME-2B data are generally consistent in terms of seasonal and latitudinal changes. However, there are also a number of noticeable differences. One can see from the GOME-2A time series that a change in VCD levels happens in late 2013-early 2014 with increasing trends depending on the latitudes, in particular in the Northern hemisphere. It is not clear whether it corresponds only to the degradation of the instrument or if effects due to the change in GOME-2A resolution (reduced swath) also contribute. The GOME-2B results are in general good agreement with the VCD levels of the GOME-2A data before the switch to improved resolution. However, at mid-latitudes, the differences appear more pronounced. Finally, Fig. 7 (bottom panel) shows the time-series for total BrO SCDs and suggests that observed differences are due to a combination of differences from the spectral fitting/sampling of data and the stratospheric correction and AMFs.



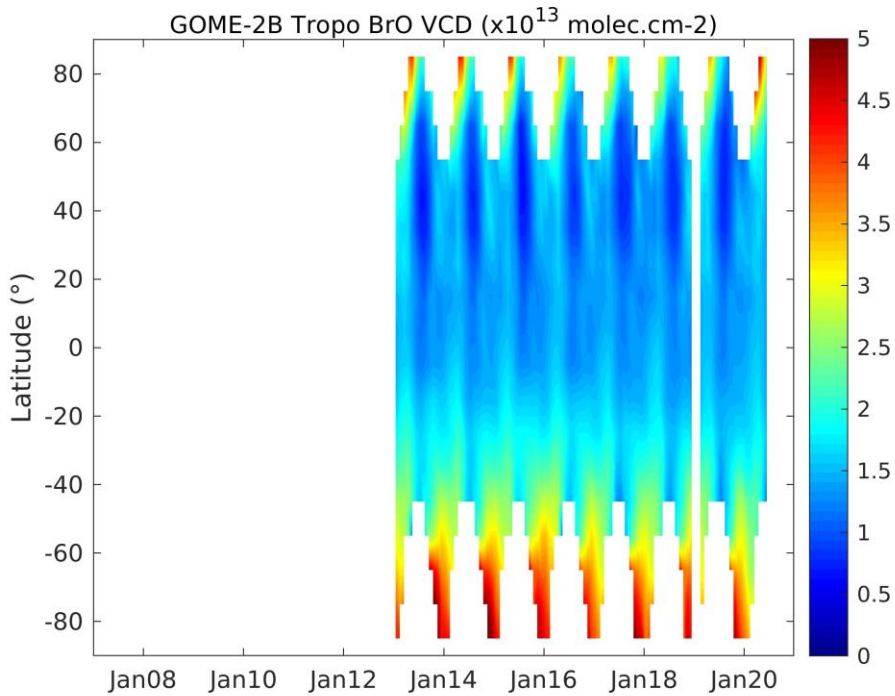
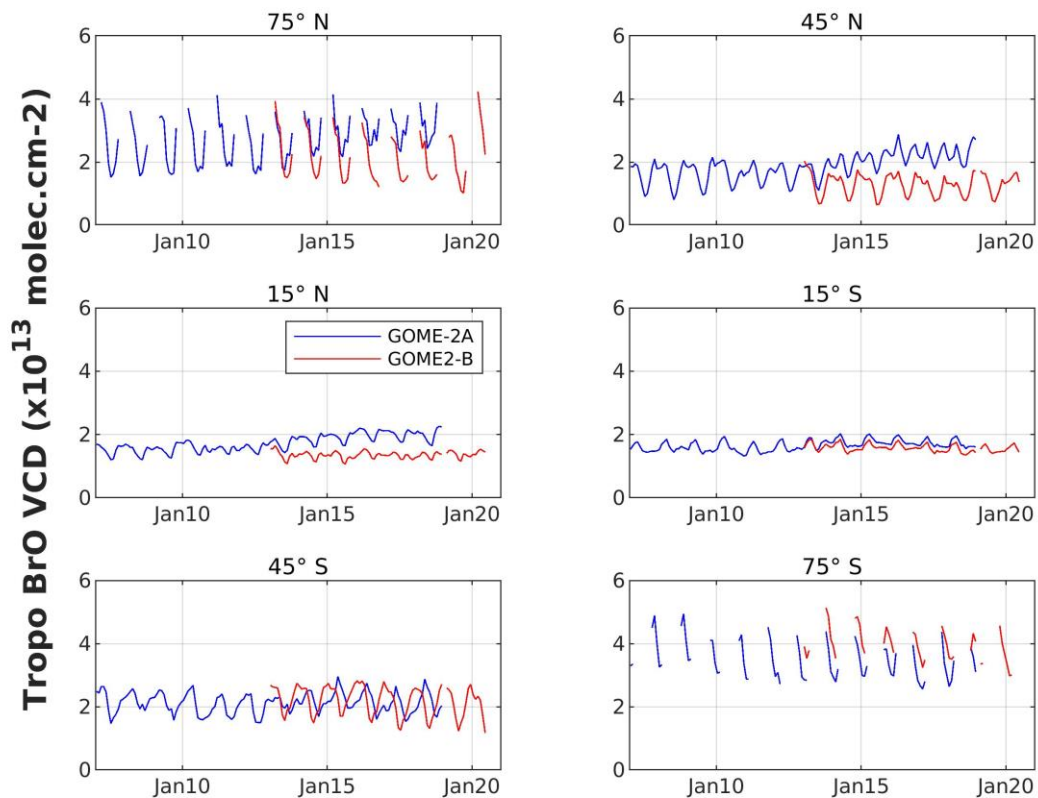


Figure D.6: Comparison of time-series of daily averaged tropospheric BrO columns (for 5° zonal bands) from GOME-2A (top) and GOME-2B (bottom) from 2007 to June 2020.



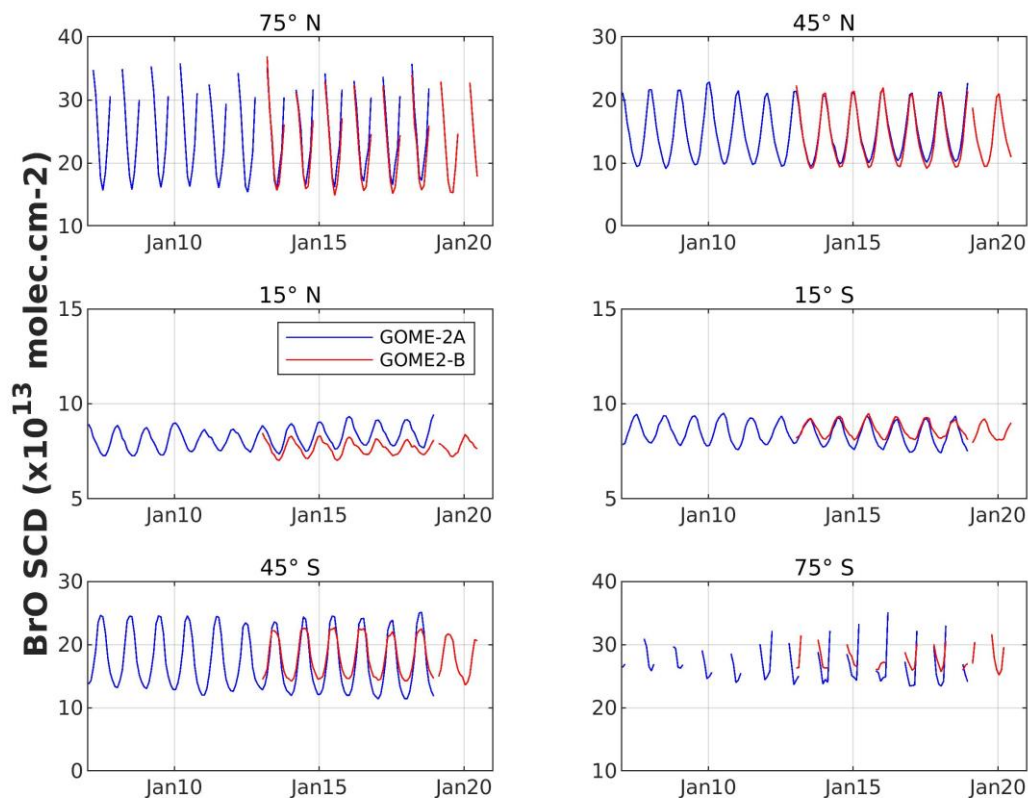


Fig D.7: Comparison of time-series of daily averaged tropospheric BrO vertical columns (top panel, same as Fig. 6) and total BrO slant columns (bottom panel) from GOME-2A and GOME-2B from 2007 to June 2020, for a selection of zonal bands.

E. COMPARISONS WITH GROUND-BASED MEASUREMENTS

E1. Ground-based DOAS data sets description

We assess tropospheric BrO vertical column densities (VCDs) generated using the G2_L2_BrOTrop processor through comparisons with ground-based DOAS measurements from IUP-HD, UAF, and BIRA-IASB. In the Northern Hemisphere, these measurements were performed at Utqiagvik (formerly known as Barrow), in the Arctic Ocean from several mobile platforms, and at Harestua (Norway). In Antarctica, these measurements were performed at Neumayer and Arrival Height. Except at Harestua, all the ground-based measurements were performed using MAX-DOAS instruments and analyzed with the HeiPrO code (Frieß et al., 2011), which implements an optimal estimation method (OEM) to retrieve the profile information. Regarding Harestua, the BIRA-IASB zenith-only DOAS measurements were analyzed according to the methods described by Hendrick et al. (2007). This Harestua retrieval scheme also applies an OEM to retrieve the tropospheric and stratospheric BrO content. Note that Zenith-only DOAS measurements are less sensitive than MAX-DOAS to the lower troposphere. On the other hand, Zenith measurements can be more sensitive to the free troposphere than MAX-DOAS. In our case, the MAX-DOAS measurements in the Arctic represent the BrO VCDs from the surface to 2km above ground level.

The measurements in the Arctic reveal the global maxima of BrO, which occurs in spring with the bromine explosions above young sea ice. These events are not detected at Harestua, which is more representative for the background tropospheric BrO levels.

Place	Group	Time Period	Instrument	Reference
Utqiagvik - ex Barrow (71.32°N, 156.67°W)	IUP	26/02/2009 - 16/04/2009	MAX-DOAS	Frieß et al. (2011)
Utqiagvik - ex Barrow (71.32°N, 156.67°W)	UAF	2012 -2016	MAX-DOAS	Simpson et al. (2017)
Arctic Ocean (O-buoys and IceLander)	UAF	2011-2016	MAX-DOAS	Simpson et al. (2017)
Harestua (60.21°N, 10.75°E)	BIRA-IASB	2013-2020	Zenith-only DOAS	Hendrick et al. (2007)
Neumayer (70.66°S, 8.25 W)	IUP	2007-2019	MAX-DOAS	Frieß, personal communication (2021)

Arrival Height (77.83°S, 166.67°E)	IUP	2012-2019	MAX-DOAS	Frieß, personal communication (2021)
---------------------------------------	-----	-----------	----------	--

Table E.1.: Ground-based DOAS observations included in this validation exercise.

Table E.1 presents the ground-based measurements used in this validation exercise including the timespan. Note that the Arctic BrO measurements only cover the spring season, i.e. when the tropospheric BrO VCDs are maximal. Figure E.1 shows the location of the Arctic BrO measurements in the Arctic Ocean.



Figure E.1: Locations and tracks of the ground-based measurements in the Arctic Ocean.

E2. Coincidence criteria

For the MAX-DOAS data in the Arctic and Antarctic, we average the GOME-2 pixels within a radius of 50 km around a ground-based measurements, which we average during 2 hours around the satellite overpasses (+/- 1h). In this validation dataset, it is common to have several orbits for the same day.

For Harestua, the BrO VCDs are generally lower and we average within 150 km to reduce the noise. We also consider monthly-averaged values.

We have tested different thresholds for the SZA and ground-based measured AOD (the latter only in the Arctic, as it is not available for Harestua). This impacts the numerical values (regression parameters and correlation) of individual datasets but not the overall picture described in the following.

E3. Comparison results in Arctic and at Harestua

E.3.1 Arctic MAX-DOAS measurements

Figure E.2 and E.3 compare GOME-2A and MAX-DOAS tropospheric BrO VCD measured at Utqiagvik (formerly known as Barrow) in Spring 2009. The first figure shows the two satellite products described in section C (operational and scientific). The dynamic range of the satellite measurements is larger than its ground-based counterpart, which is expected from the larger noise of the spaceborne measurements. However, the three datasets are clearly correlated, which is quantified in figures E.3 and E.4.

Overall, the scient product appears slightly less biased and more correlated with respect to the ground-based dataset. The difference is however small, and the two satellite products are close to each other, with a slope of 0.84 and a correlation coefficient of 0.9.

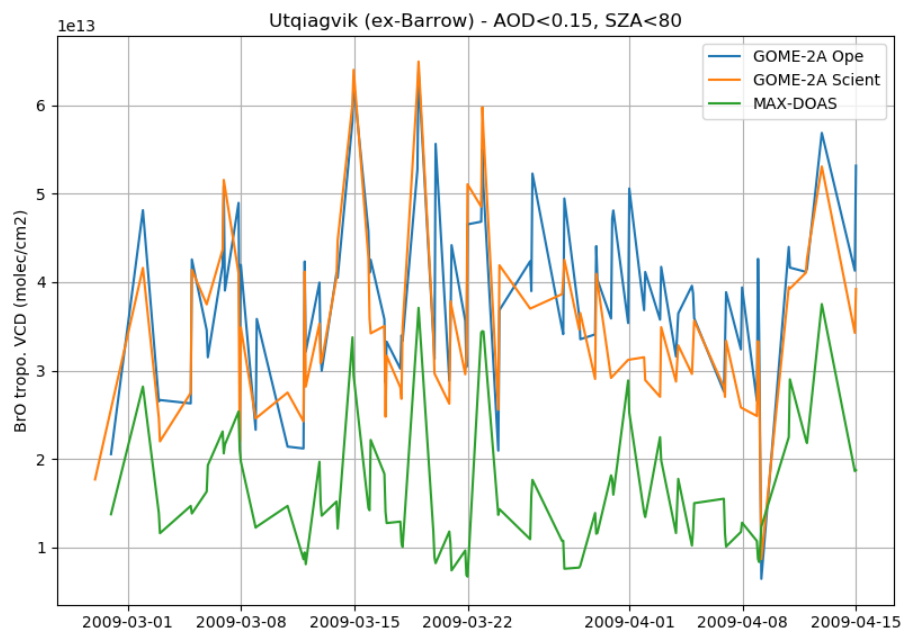


Figure E.2.: Time series of the MAX-DOAS and coincident ($\pm 1h$, $\pm 50 km$) GOME-2A tropospheric BrO VCD measurements at Utqiagvik in Spring 2009

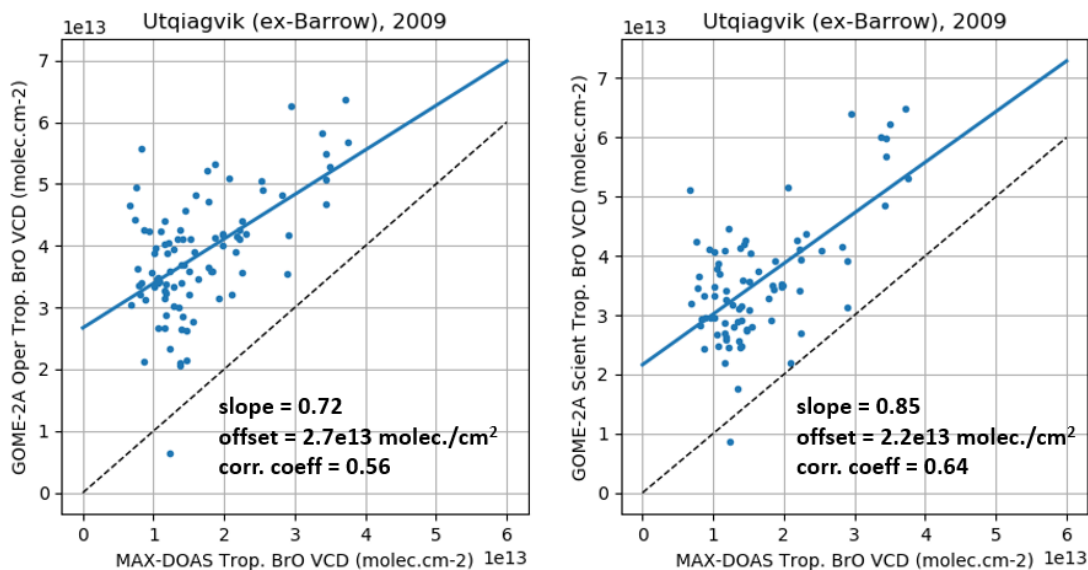


Figure E.3: Linear regression chart between MAX-DOAS and coincident ($\pm 1h$, ± 50 km) GOME-2A tropospheric BrO VCD measurements at Utqiagvik (formerly known at Utqiagvik) in Spring 2009 for oper (left) and scient (right) GOME-2A products.

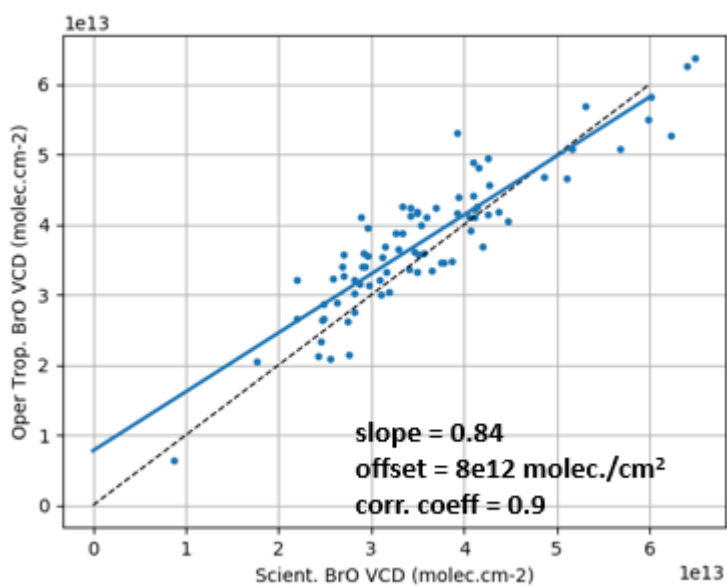


Figure E.4 : Linear regression chart between oper and scient GOME-2A products for the Barrow measurements of figs. E.2 and E.3.

We performed such comparisons between GOME-2 A and B and the set of MAX-DOAS measurements in the Arctic. Some of the results are shown in figures E.5 (Utqiagvik, 2012-2016) E.6 and E.7 (O-Buoys).

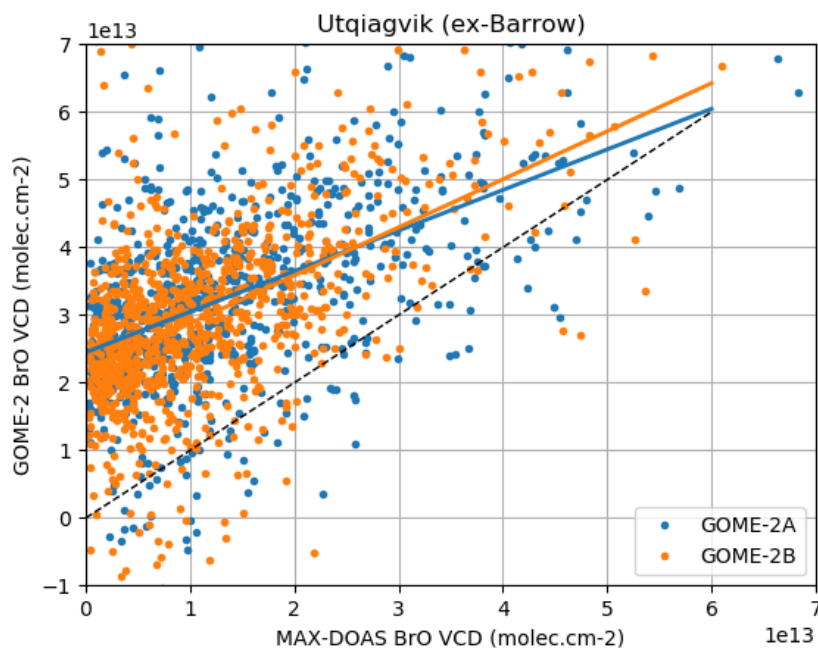


Figure E.5: Same as Fig. E.3 but for the MAX-DOAS measurements at Utqiagvik (formerly known as Barrow) between 2012 and 2016, and including the GOME-2B data.

Figure E.8 summarizes these comparison exercises. While the values are different for each datasets, the general picture is consistent with the initial findings of 2009. It reveals, for both GOME-2 instruments, slopes close to unity, correlation between 0.4 and 0.8, and offsets between 2 and 3e13 molec./cm². Note that for visibility and in figure E.6 only, we averaged daily values, which further improves the correlation between ground-based and satellite measurements.

E.3.2 Zenith-DOAS measurements in Harestua

Figure E.9 compares monthly averages of GOME-2A and B with Zenith-DOAS observations in Harestua, Norway (60.22°N, 10.75°E). For visibility, we only show the measurements recorded with a high sun (SZA < 50°).

The ground-based observations indicate a tropospheric BrO VCD between 1 and 2e13 molec.cm⁻². The GOME-2B satellite observations are close to these ground-based values, with a slightly larger dynamic range (mainly within 0.5 to 2.5 molec.cm⁻²). It appears that GOME-2A is systematically above GOME-2B from 2014, typically by 1e13 molec.cm⁻² but up to 4e13 molec.cm⁻². This could be related to the instrumental degradation of GOME-2A.

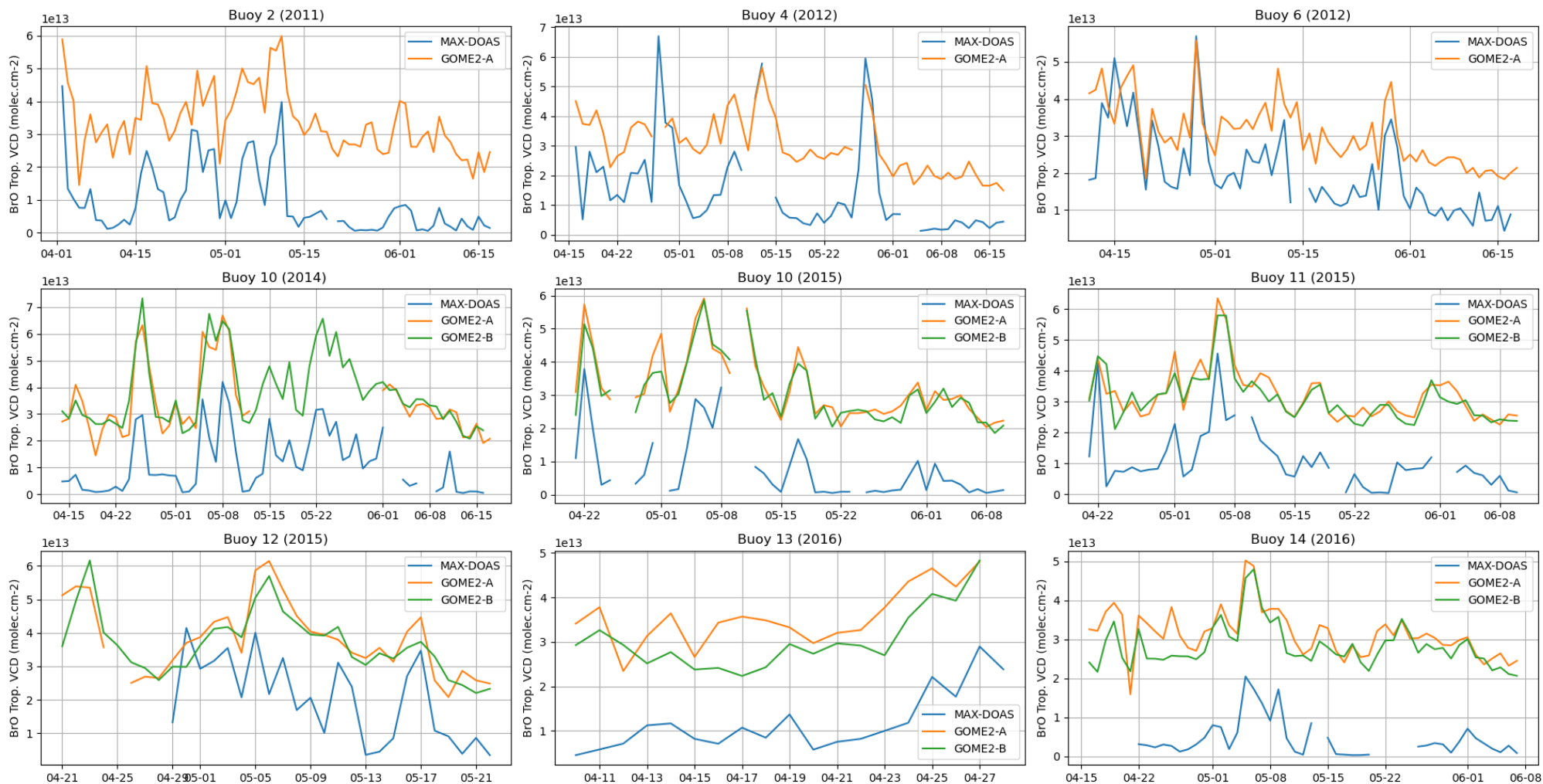


Figure E.6: Time series of the MAX-DOAS from the O-Buoys and coincident GOME-2A and GOME-2B tropospheric BrO VCD measurements in the Arctic between 2011 and 2016 (daily averages).

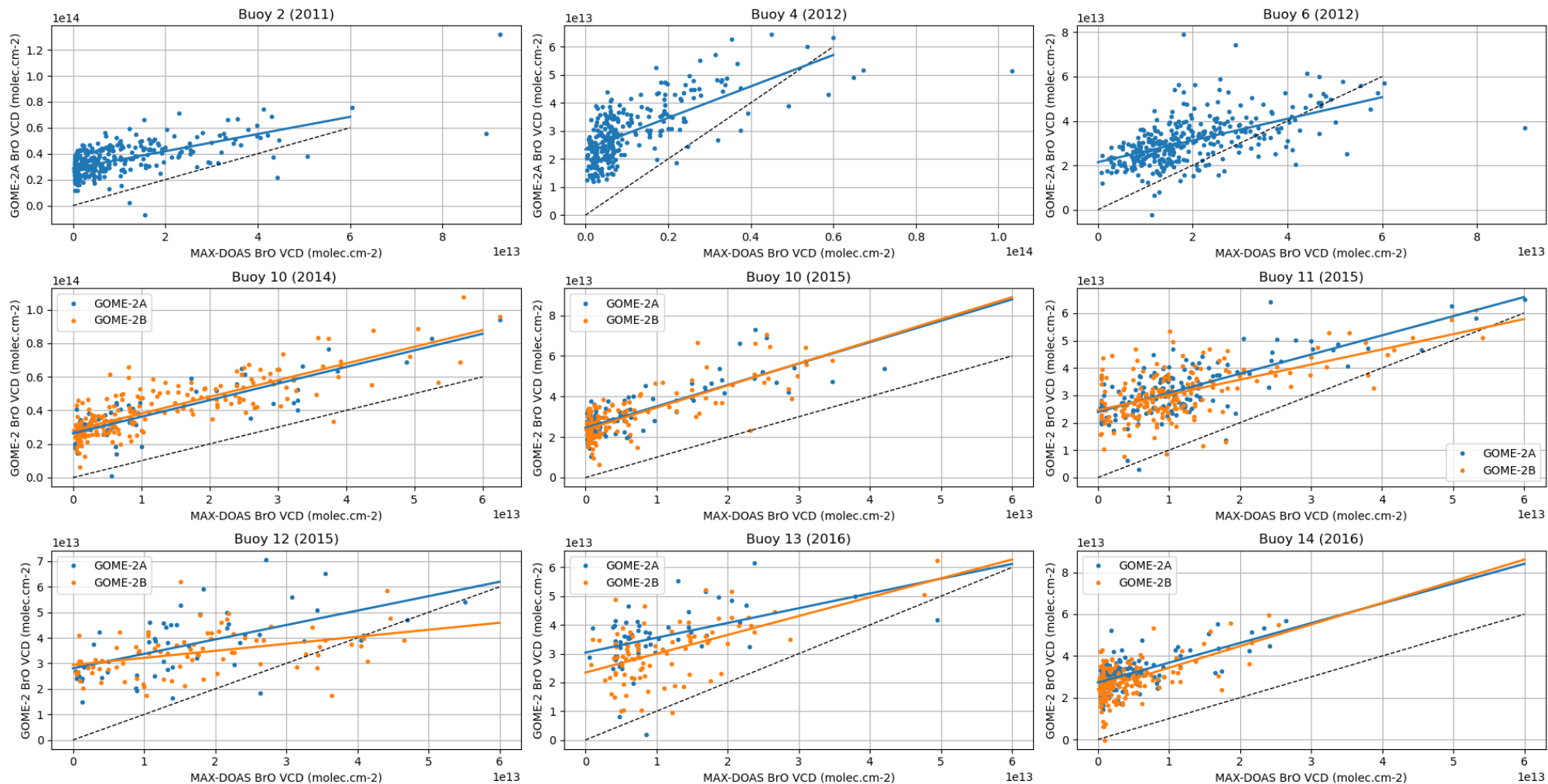


Figure E.7: Same as Fig E.3 but using the data from the MAX-DOAS measurements on the O-Buoys drifting across the Arctic between 2011 and 2016

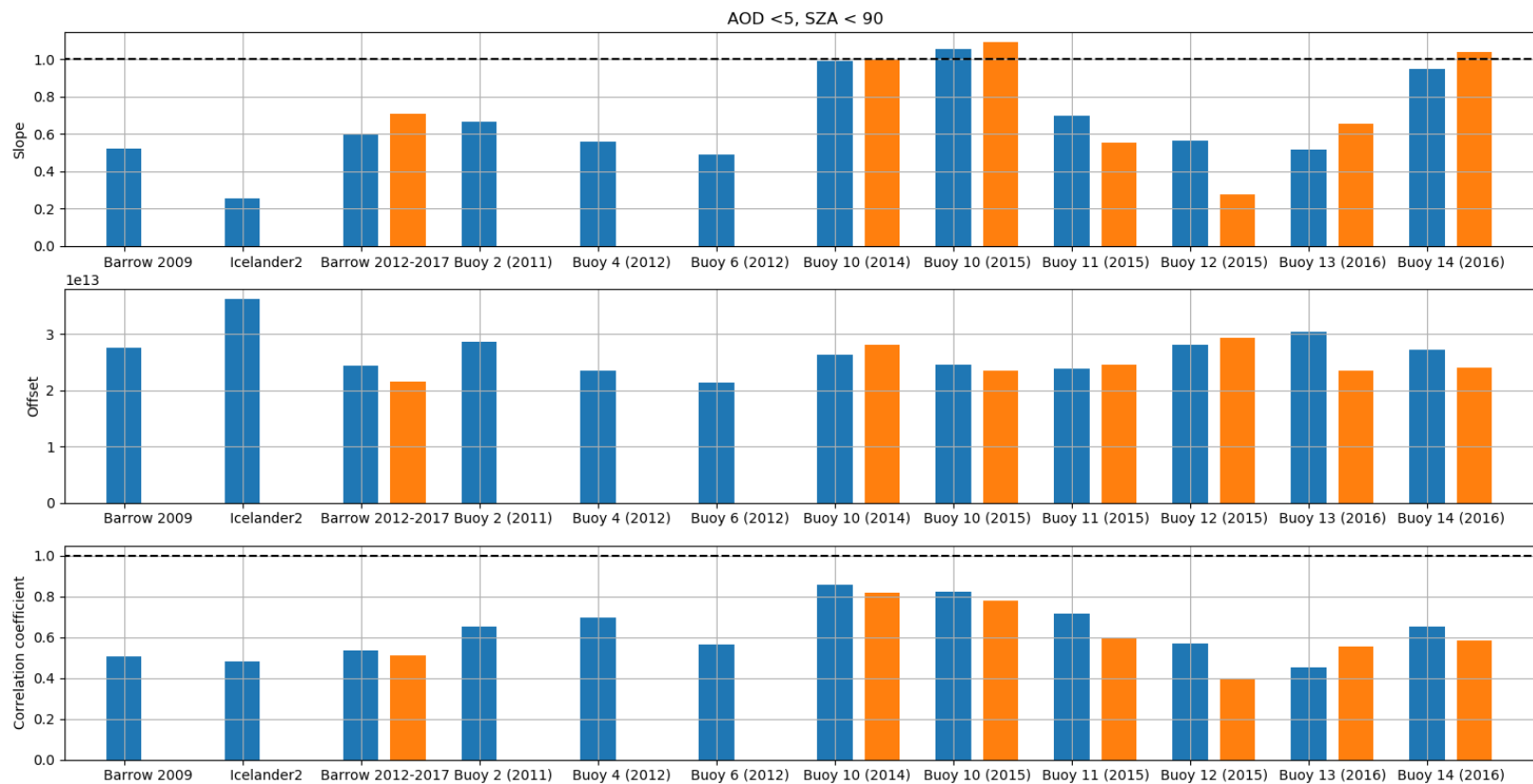


Figure E.8: Summary of the regressions and correlation coefficients of the measurements in the Arctic Ocean between 2009 and 2016. GOME2-A is in blue, GOME-2B in orange.

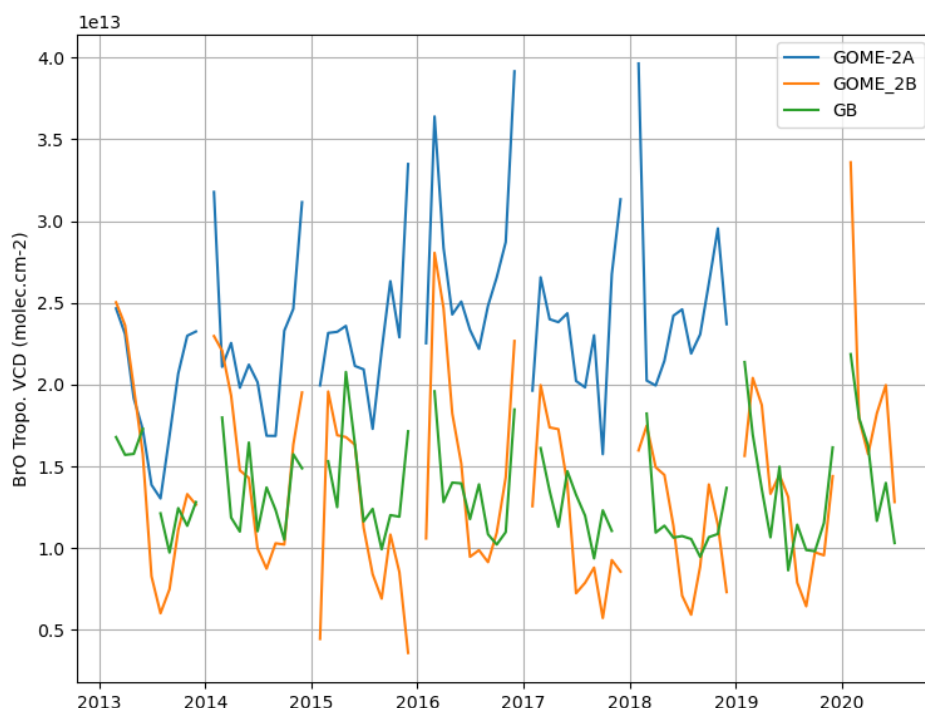


Figure E.9: Time series of the monthly averaged Zenith-DOAS and coincident (± 150 km) GOME-2A and GOME-2B tropospheric BrO VCD measurements at Harestua between 2013 and 2020. For visibility, we only show the data corresponding to $SZA < 50^\circ$.

E.3.3 Interpretation in terms of the product requirements

Since they are mainly sensitive to the lower troposphere (under 2 km altitude), the MAX-DOAS data are expected to have a low bias when compared to the satellite data, a bias which corresponds to the BrO background in the free troposphere.

The BrO vmr in the free troposphere is estimated to be around 1 ppt (Theys et al., 2011, Schmidt et al., 2016). Integrating this vmr between 2 and 8 km (taken as the tropopause altitude in Arctic Spring) altitude yields a ghost VCD of $1e13$ molec. cm^{-2} .

Based on this, we added $1e13$ molec. cm^{-2} to the MAX-DOAS measurements in Arctic to investigate how the GOME-2 product fits the requirements. On the other hand, the measurements at Harestua are in zenith geometry and are in principle sensitive to the full troposphere. Therefore, no correction was added to the Harestua ground-based data. Note that our estimate of $1e13$ molec. cm^{-2} appears consistent with the measurements in Harestua.

Figure E.10 presents the time series of relative differences between GOME-2A and corrected (adding $1e13$ molec. cm^{-2}) MAX-DOAS measurements, corresponding to the dataset of Fig. E.2. The dashed horizontal lines indicate the product requirements (Table A.1). It appears that the threshold requirements is mainly respected. On average, the relative difference is $+36\% \pm 48\%$.

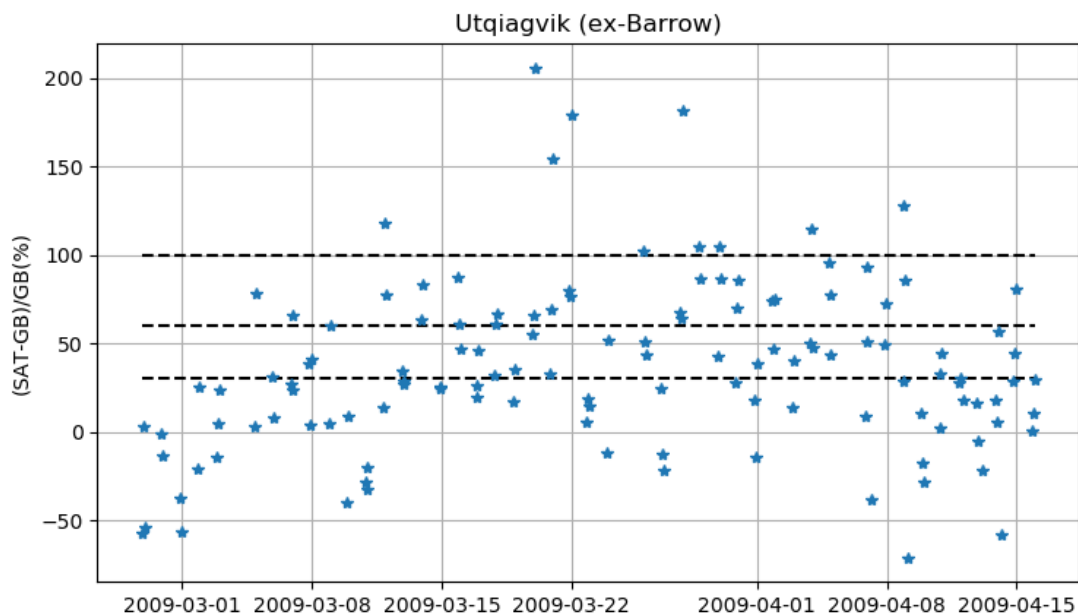


Figure E.10 Time series of the relative differences between the GOME-2A tropospheric BrO VCDs and their MAX-DOAS counterparts for the measurements in Utqiagvik (formerly known as Barrow) in Spring 2009. Note that we added $1e13 \text{ molec.cm}^{-2}$ to account for the BrO content in the free troposphere.

Figure E.11 summarizes the relative differences for the corrected Arctic dataset. It confirms a high bias of the satellite compared to the ground based data, but on average the satellite measurements meet the threshold requirements.

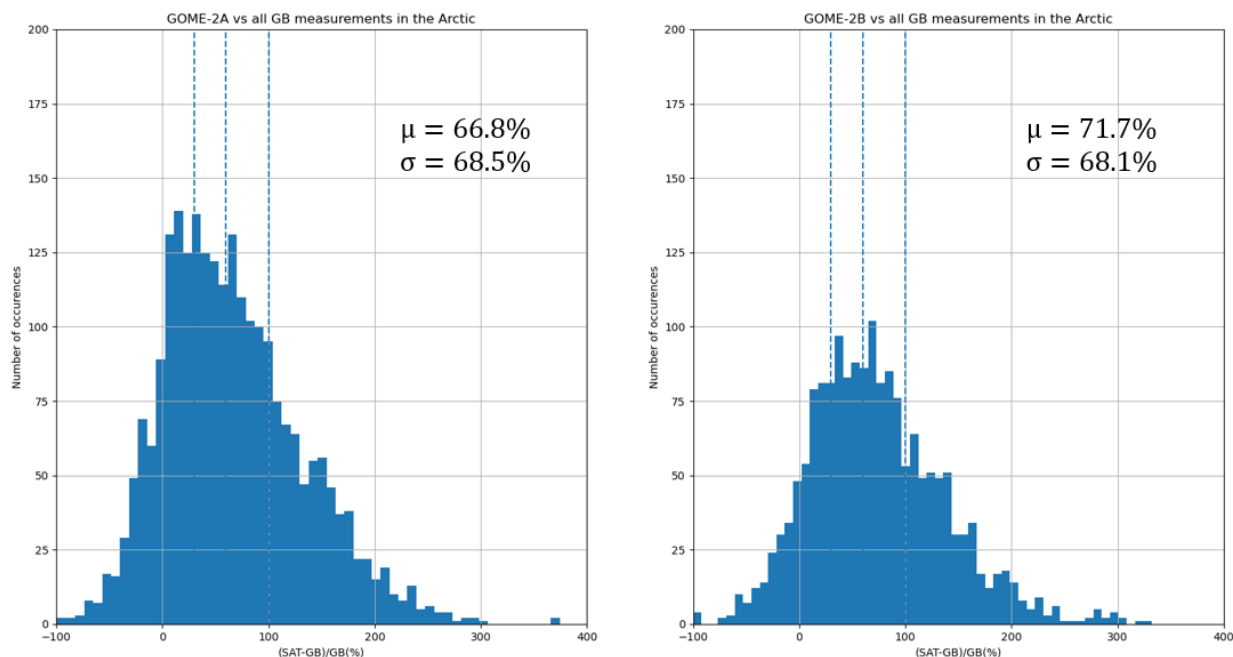


Figure E.11 Distributions of the relative differences between satellite and ground-based measurements in the Arctic between 2012 and 2016.

Note that the comparisons with the MAX-DOAS data depend on our assumptions on the ghost BrO VCD in the free troposphere. The GOME-2 product would better fit its requirements with a larger ghost column. It is therefore particularly interesting to look to the comparison at Harestua, where the ground-based measurements are sensitive to the whole troposphere.

Figure E.12 shows the times series of the relative differences between satellite and ground-based measurements in Harestua. The threshold requirements is respected on average for the two GOME-2 instruments but the aforementioned GOME2-A drift is visible from 2014, possibly linked with the instrumental degradation. For this period, the mean relative differences are 84% and 1% for GOME-2A and GOME-2B, respectively.

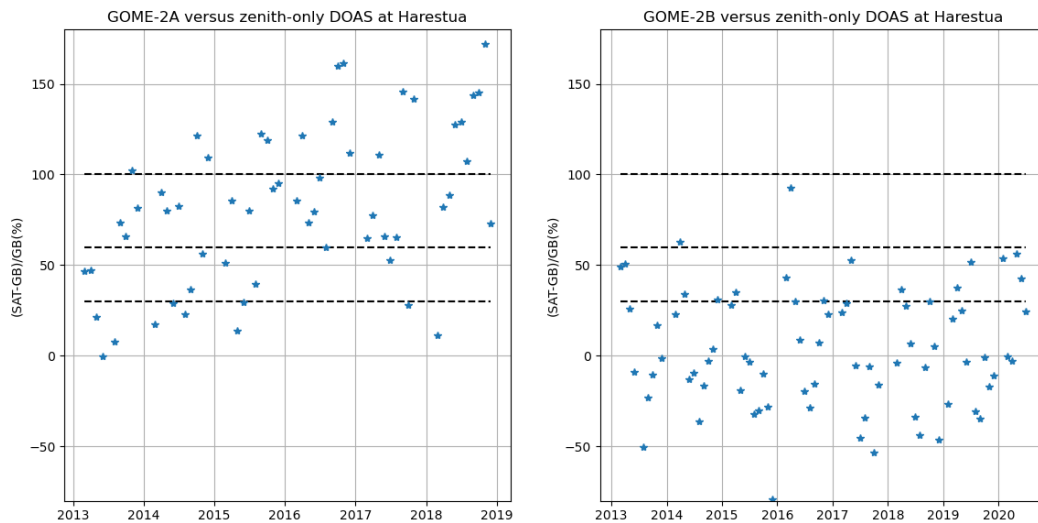


Fig E.12 Time series of the relative differences between GOME-2A (left) and GOME-2B (right) over Harestua.

E4. Comparison results in Antarctica

Figure E.13 shows the location of the two MAX-DOAS stations in Antarctic. The GOME-2 measurements of tropospheric BrO VCDs above these two sites are compared in Figures E.14 and Figures E.15.

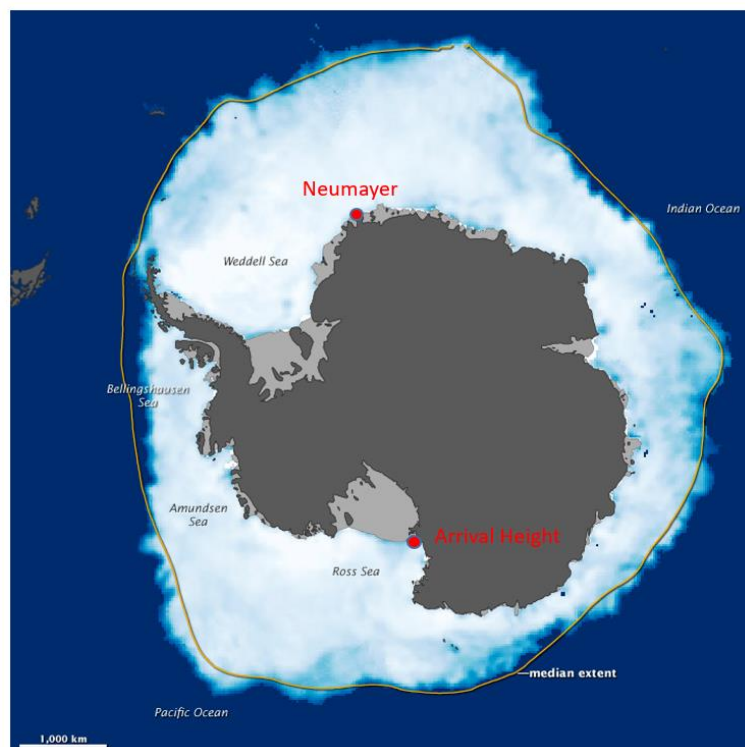


Figure E.13 Locations of ground-based MAX-DOAS in Antarctica, with sea ice extent on 26 September 2012 (NASA Earth observatory).

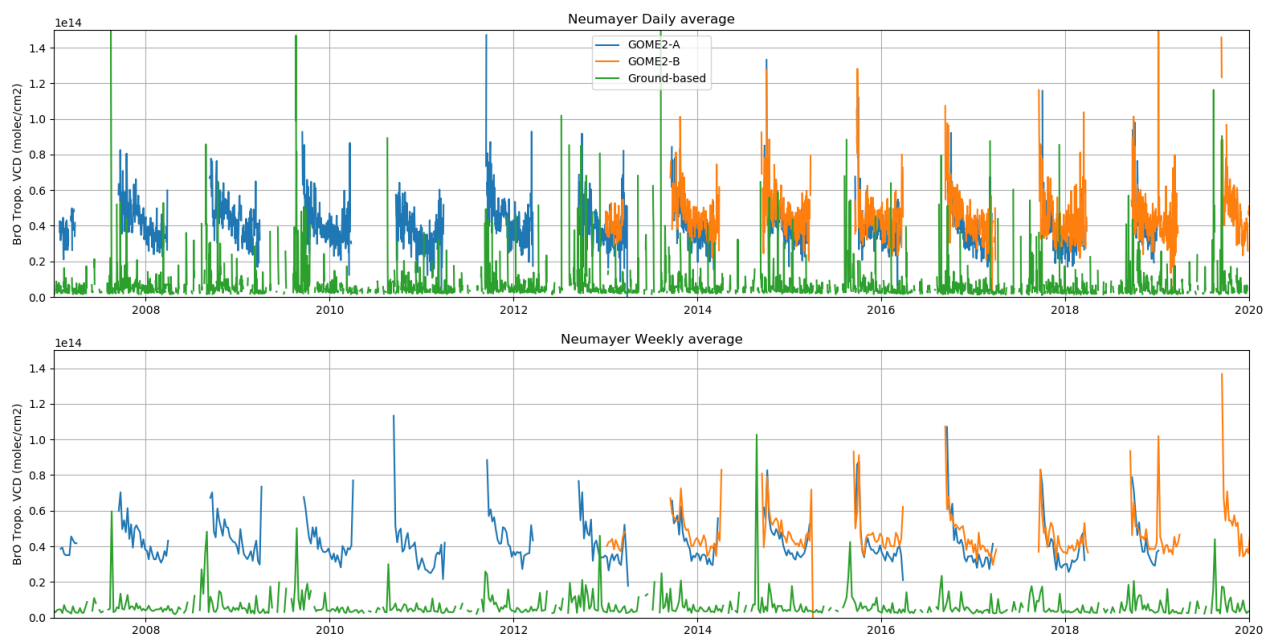


Figure E.14 Time series of the daily and weekly average MAX-DOAS and coincident GOME-2 measurements of tropospheric BrO VCDs at Neumayer.

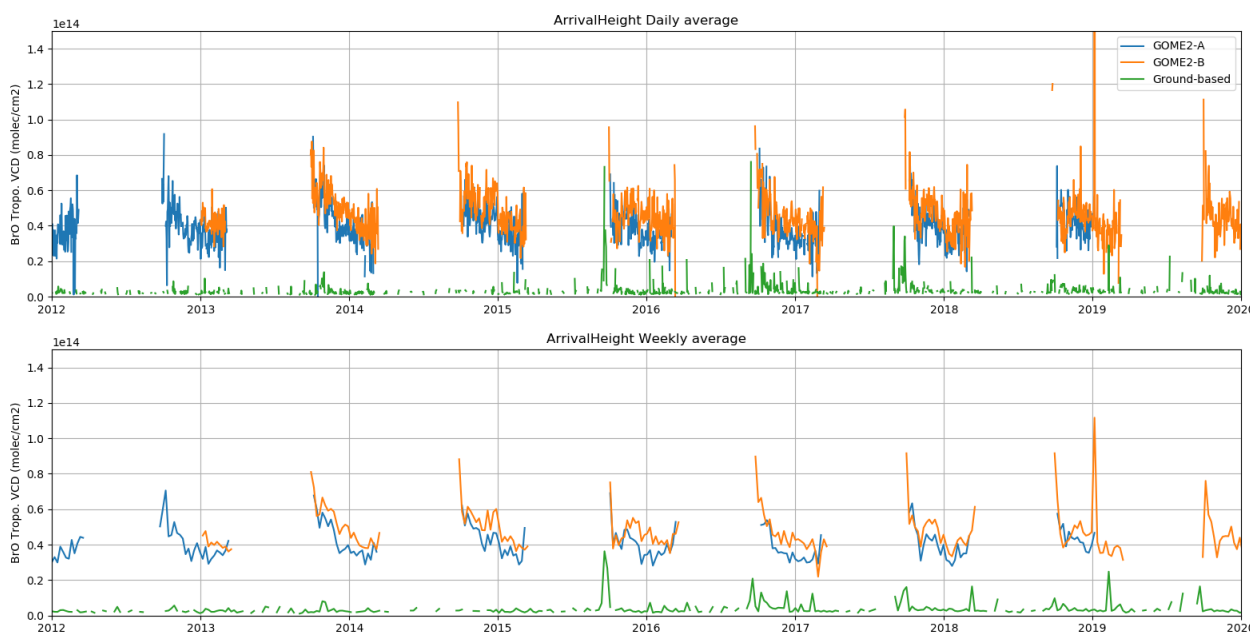


Figure E.15 Same as Figure E.14 but at Arrival Height.

These comparisons, while also showing elevated levels of BrO in spring, appear significantly different from the ones in Arctic shown in section E.3. First, the offset between the ground-based and satellite products appears less stable. This offset is large in austral spring (September), when it is around 6×10^{13} molec. cm^{-2} , decreases to 3×10^{13} molec. cm^{-2} in February, when it often starts again to increase until April. The correlation between the satellite and MAX-DOAS products is significantly weaker than in Arctic, with correlation coefficients around 0.3.

We believe that both dataset are valuable and that the vertical distribution of BrO in the troposphere explain the observed differences.

Indeed, as discussed in Section C, the GOME-2 tropospheric BrO VCDs around Antarctica shown on Figures E.14 and E.15 are consistent with the scientific product described by Theys et al. (2011), with a small positive bias of around $1e13$ molec.cm⁻².

Considering the MAX-DOAS VCDs, they are retrieved with the same algorithms as the one used in Arctic shown in Section E.3. Moreover, the MAX-DOAS measurements in Neumayer are consistent with ground concentrations derived from a Longpath-DOAS instrument (Nasse et al., 2019).

Such a discrepancy between MAX-DOAS and GOME-2 measurements in Antarctica was reported before at Halley (Roscoe et al., 2009). The authors concluded that most of the BrO was in the free troposphere. This finding and in general the observations of Roscoe et al. at Halley are consistent with the comparisons shown in this report, as the MAX-DOAS measurements are mainly sensitive to the lower part of the troposphere.

To verify this assumption, one could try to apply the OEM algorithm used for the zenith-only DOAS data of Harestua to the Antarctic ground-based measurements. Tropospheric BrO columns derived with this algorithm would be representative of the full troposphere, and thus would help to confirm the free tropospheric BrO loading and further characterize the GOME-2 measurements in Antarctica. To achieve that, the sampling of zenith measurements around twilight should be increased, at least for the Neumayer station.

Finally, one would need to explain the profile difference between Arctic and Antarctic. One possible reason is the locations of the BrO sources compared to the stations. The Antarctic stations considered here are on the Antarctic continent, further away from the young sea-ice in Spring than e.g. Barrow is. From the Copernicus Sea-Ice data (<https://climate.copernicus.eu/sea-ice>), moreover the sea ice extent seems to follow the offset seasonality. Investigating these questions require further studies which are outside the scope of this validation report.

CONCLUSIONS

This document reports on the validation of AC-SAF GOME-2A and GOME-2B BrO tropospheric column data products retrieved at DLR with versions 1 of the GOME-2 tropospheric BrO processor (G2_L2_BrOTrop), using level-1B-R1 data based on level-0-to-1B processor version 6.3. The operational version of GOME-2 BrO tropospheric column data were compared with the scientific version of the algorithm, as well as with ground-based observations.

We have evaluated GOME-2A and GOME-2B tropospheric BrO VCDs by comparing the operational product with (1) a scientific version of the VCDs using the same GOME-2 Level-1 data, (2) ground-based measurements performed in the Arctic Ocean, in Harestua (Norway), and in Antarctica.

The main conclusions from the inter-satellite comparisons are:

- The optimal requirements (30%) do not fit in the theoretical error budget.
- The AC SAF data record is highly correlated with the BIRA scientific product, which covers the period between January 2007 and October 2009. The differences are mainly in the range of -0.5 to $+0.5 \times 10^{13}$ molec/cm² (mean difference of $+0.5 \times 10^{12}$ molec/cm²). This corresponds to relative differences in the range of -40 to +50% (mean difference of +4%).
- Highest relative differences with respect to the scient product on the DLR tropospheric BrO VCDs mostly occur in background areas and Antarctica.
- GOME-2A and GOME-2B data are generally consistent in terms of seasonal and latitudinal changes. However, the GOME-2A time series seems to change from 2014, possibly due to instrumental degradation.

The main conclusions from the comparisons with ground-based data are:

- The GOME-2 BrO VCDs shows a good correlation with the ground-based DOAS measurements in Arctic. Linear regression analyses between the two products typically yield slopes close to unity, however there remains a small positive bias of the GOME-2 VCDs. Due to the limitation of the MAX-DOAS technique in the free troposphere, it is difficult to quantify accurately the bias, but assuming a free tropospheric BrO loading of $1e13$ molec/cm², the threshold requirement is respected with a positive bias around 70%.
- In Harestua, the average positive bias in the considered period (2013-2020) is 84% and 1%, respectively for GOME-2A and GOME-2B. The threshold requirement is respected.
- In Antarctica, the comparisons with two MAX-DOAS is more difficult to interpret, but the overall consistency and previous studies suggests that a higher fraction on the column may lie in the free troposphere and not visible with the MAX-DOAS instruments.

With respect to the available validation data, GOME-2A and GOME-2B seems to comply with the threshold requirements of 100% and appear close to the target requirements of 60%. We propose to further investigate the situation in Antarctic, e.g. by applying OEM algorithms for zenith-only DOAS measurements on historic MAX-DOAS data.

F. REFERENCES

G.1. Applicable documents

- [ATBD] Algorithm Theoretical Basis Document for GOME-2 tropospheric Bromine Monoxide columns, SAF/AC/DLR/ATBD/BrOTrop/01, Iss. 1/B, Heue et al., Dec 2020[PUM] Product User Manual of GOME-2 tropospheric BrO product, SAF/AC/DLR/PUM/BrOTrop/01, Iss 1A., Heue et al. Dec 2020
- [PRD] Service Specification Document, SAF/AC/FMI/RQ/SESP/001/issue 1.3, Hovila, J., Hassinen, S., 17 June 2019, https://acsaf.org/docs/AC_SAF_Service_Specification.pdf
- [VIM] Joint Committee for Guides in Metrology (JCGM/WG 2) 200:2008 & ISO/IEC Guide 99-12:2007, International Vocabulary of Metrology – Basic and General Concepts and Associated Terms (VIM), <http://www.bipm.org/en/publications/guides/vim.html>
- [GUM] Joint Committee for Guides in Metrology (JCGM/WG 1) 100:2008, Evaluation of measurement data – Guide to the expression of uncertainty in a measurement (GUM), http://www.bipm.org/utis/common/documents/jcgm/JCGM_100_2008_E.pdf

G.2. Reference

G.2.1 Peer-reviewed articles

- Koelemeijer, R. B. A., de Haan, J. F., and Stammes, P.: A database of spectral surface reflectivity in the range 335-772 nm derived from 5.5 years of GOME observations, *J. Geophys. Res.-Atm.*, 108(D2), 4070, doi: 10.1029/2002JD002429, 2003.
- Theys, N., Van Roozendael, M., Hendrick, F., Yang, X., De Smedt, I., Richter, A., Begoin, M., Errera, Q., Johnston, P. V., Kreher, K., and De Mazière, M.: Global observations of tropospheric BrO columns using GOME-2 satellite data, *Atmos. Chem. Phys.*, 11, 1791-1811, 2011.
- Tilstra, L. G., O. N. E. Tuinder, P. Wang, and P. Stammes (2017), Surface reflectivity climatologies from UV to NIR determined from Earth observations by GOME-2 and SCIAMACHY, *J. Geophys. Res. Atmos.*, 122, 4084–4111, doi:10.1002/2016JD025940
- Wang, P., Stammes, P., van der A, R., Pinardi, G., and Van Roozendael, M.: FRESKO+: an improved O₂ A-band cloud retrieval algorithm for tropospheric trace gas retrieval, *Atmos. Chem. Phys.*, 8, 6565-6576, 2008.
- Peterson, P. K., Simpson, W. R., Pratt, K. A., Shepson, P. B., Frieß, U., Zielcke, J., Platt, U., Walsh, S. J., and Nghiem, S. V.: Dependence of the vertical distribution of bromine monoxide in the lower troposphere on meteorological factors such as wind speed and stability, *Atmos. Chem. Phys.*, 15, 2119-2137, doi:10.5194/acp-15-2119-2015, 2015.
- Hendrick, F., M. Van Roozendael, M. P. Chipperfield, M. Dorf, F. Goutail, X. Yang, C. Fayt, C. Hermans, K. Pfeilsticker, J.-P. Pommereau, J. A. Pyle, N. Theys, and M. De Mazière, Retrieval of stratospheric and tropospheric BrO profiles and columns using ground-based zenith-sky DOAS observations at Harestua, 60°N, *Atmospheric Chemistry and Physics*, 7, 4869-4885, 2007

Frieß, U., Sihler, H., Sander, R., Pöhler, D., Yilmaz, S., & Platt, U. (2011). The vertical distribution of BrO and aerosols in the Arctic: Measurements by active and passive differential optical absorption spectroscopy. *Journal of Geophysical Research*, 116, D00R04. <https://doi.org/10.1029/2011JD015938>

Simpson, W. R., Peterson, P. K., Frieß, U., Sihler, H., Lampel, J., Platt, U., Moore, C., Pratt, K., Shepson, P., Halfacre, J., and Nghiem, S. V.: Horizontal and vertical structure of reactive bromine events probed by bromine monoxide MAX-DOAS, *Atmos. Chem. Phys.*, 17, 9291–9309, <https://doi.org/10.5194/acp-17-9291-2017>, 2017.

Peterson, P. K., Pöhler, D., Sihler, H., Zielcke, J., General, S., Frieß, U., Platt, U., Simpson, W. R., Nghiem, S. V., Shepson, P. B., Stirm, B. H., Dhaniyala, S., Wagner, T., Caulton, D. R., Fuentes, J. D., and Pratt, K. A.: Observations of bromine monoxide transport in the Arctic sustained on aerosol particles, *Atmos. Chem. Phys.*, 17, 7567–7579, <https://doi.org/10.5194/acp-17-7567-2017>, 2017.

Knepp, T. N., Bottenheim, J., Carlsen, M., Carlson, D., Donohoue, D., Friederich, G., Matrai, P. A., Natcheva, S., Perovich, D. K., Santini, R., Shepson, P. B., Simpson, W., Valentic, T., Williams, C., and Wyss, P. J.: Development of an autonomous sea ice tethered buoy for the study of ocean-atmosphere-sea ice-snow pack interactions: the O-buoy, *Atmos. Meas. Tech.*, 3, 249–261, <https://doi.org/10.5194/amt-3-249-2010>, 2010.

Schmidt, J. A., Jacob, D. J., Horowitz, H. M., Hu, L., Sherwen, T., Evans, M. J., Liang, Q., Suleiman, R. M., Oram, D. E., Le Breton, M., Percival, C. J., Wang, S., Dix, B., Volkamer, R. . (2016), Modeling the observed tropospheric BrO background: Importance of multiphase chemistry and implications for ozone, OH, and mercury, *J. Geophys. Res. Atmos.*, 121, 11,819–11,835, doi:10.1002/2015JD024229.

Nasse, J.-M., Eger, P. G., Pöhler, D., Schmitt, S., Frieß, U., and Platt, U.: Recent improvements of long-path DOAS measurements: impact on accuracy and stability of short-term and automated long-term observations, *Atmos. Meas. Tech.*, 12, 4149–4169, <https://doi.org/10.5194/amt-12-4149-2019>, 2019.

Roscoe, H. K., Brough, N., Jones, A. E., Wittrock, F., Richter, A., Van Roozendaal, M., & Hendrick, F. (2009). Characterisation of vertical BrO distribution during events of enhanced tropospheric BrO in Antarctica, from combined remote and in-situ measurements. *Journal of Quantitative Spectroscopy and Radiative Transfer*, 138, 70–81. <https://doi.org/10.1016/J.JQSRT.2014.01.026>

APPENDIX 1/ OPERATIONAL AND SCIENTIFIC ALGORITHM SETTINGS

	Oper (left) vs Scient (right)	
BrO slant column: DOAS fit+equatorial correction	<p>Sun spectrum as reference</p> <p>Fitted slit and online convolution</p> <p>Mean of 1 calendar-day SCD in tropical pacific set to 7.5×10^{13} molec/cm² (similar as oper)</p>	<p>Sun spectrum used as reference</p> <p>Fixed slit function</p> <p>No SCD correction</p>
BrO stratospheric column	Input O3 and NO2 columns: small differences (not identical versions)	
	<p>Tropopause height:</p> <p>ERA-5 3.5 PVU level at high latitude and 380K potential temperature in the tropical band, latitude weighted mean between 25° and 50°.</p>	<p>Tropopause height:</p> <p>ERA-Interim 3.5 PVU level and 380K potential temperature in the tropical band if dynamical tropopause height is higher.</p>
BrO stratospheric AMF	None, except differences in BrO profiles and tropopause height (see above)	
BrO tropospheric AMF	<p>Surface albedo:</p> <p>Tilstra et al 2017 (GOME_2 version3) DLER including scanangle dependency</p> <p>Profile: For albedo <0.5: a gaussian profile at 6 km with 3km FWHM</p> <p>for albedo>0.5 a box profile up to 2.5 km</p>	<p>Surface albedo:</p> <p>Koelemeijer et al. (2003)</p> <p>Profile: 1 km box for albedos>0.5</p> <p>Constant in the free troposphere for albedos <0.5</p>
	<p>Cloud product:</p> <p>OCRA/ROCINN CRB (operational), retrieved parameters are cloud fraction, cloud albedo, cloud height.</p> <p>Cloud filtering : 0-0.5 cloud</p>	<p>Cloud product: FRESCO+ (Wang et al., 2008), retrieved parameters are cloud fraction, cloud height (cloud albedo fixed to 0.8).</p>

	<p>fraction.</p> <p>An effective height is calculated, if the effective height is below 700m above surface and the albedo is higher than 0.5 then the effective height is set to the surface.</p> <p>Treatment of snow/ice: Snow: ECMWF (ERA-5) reanalysis, including snow albedo. Ice: OSI-SAF daily sea ice maps, assumed ice albedo of 0.9.</p> <p>The final surface albedo is a weighted average of snow/ice albedo and water albedo (0.06), with a weight equal to snow/ice fraction. For snow/ice free scenes, albedo of 0.05 is used (if the climatological albedo is larger than 0.5).</p>	<p>Cloud filtering : 0-0.4 cloud fraction.</p> <p>Treatment of snow/ice: Switch to FRESCO+ snow/ice mode, i.e. use retrieved scene albedo as surface albedo, if the difference between the surface pressure and the retrieved cloud top pressure is below 120 mbar. In FRESCO+ nominal mode, surface albedo of 0.8 is used for pixels with a cloud fraction larger than 0.7 and with a pressure difference between the surface and the top of the cloud smaller than 150 mbar.</p>
--	--	--

APPENDIX 2/ CHANGES WITH RESPECT TO THE PREVIOUS VERSION

This appendix summarizes the changes introduced compared to the previous version of the AC-SAF data record for GOME-2 tropospheric BrO, which was not fulfilling the threshold requirements.

	Version 1	Version 2 (this one)
1	Earth shine as reference	Solar reference
2	Serdyuchenko et al ozone cross section	BDM ozone cross section
3	Apriori Profile up to 1 km	Apriori profile up to 2.5 km
4	Tropopause interpolated between 25° and 50° latitude	Tropopause interpolated between 20° and 45° latitude